

Fall 12-2016

Modern Fair-Weather and Storm Sediment Transport Around Ship Island, Mississippi: Implications for Coastal Habitats and Restoration Efforts

Eve Rettew Eisemann
University of Southern Mississippi

Follow this and additional works at: https://aquila.usm.edu/masters_theses

 Part of the [Environmental Health and Protection Commons](#), [Environmental Indicators and Impact Assessment Commons](#), [Environmental Monitoring Commons](#), [Geology Commons](#), [Geomorphology Commons](#), [Natural Resources and Conservation Commons](#), [Natural Resources Management and Policy Commons](#), [Numerical Analysis and Computation Commons](#), [Oceanography Commons](#), [Other Applied Mathematics Commons](#), [Sedimentology Commons](#), [Stratigraphy Commons](#), [Sustainability Commons](#), and the [Terrestrial and Aquatic Ecology Commons](#)

Recommended Citation

Eisemann, Eve Rettew, "Modern Fair-Weather and Storm Sediment Transport Around Ship Island, Mississippi: Implications for Coastal Habitats and Restoration Efforts" (2016). *Master's Theses*. 260. https://aquila.usm.edu/masters_theses/260

This Masters Thesis is brought to you for free and open access by The Aquila Digital Community. It has been accepted for inclusion in Master's Theses by an authorized administrator of The Aquila Digital Community. For more information, please contact Joshua.Cromwell@usm.edu.

MODERN FAIR-WEATHER AND STORM SEDIMENT TRANSPORT AROUND
SHIP ISLAND, MISSISSIPPI: IMPLICATIONS FOR COASTAL
HABITATS AND RESTORATION EFFORTS

by

Eve Rettew Eisemann

A Thesis
Submitted to the Graduate School
and the School of Ocean Science and Technology
at The University of Southern Mississippi
in Partial Fulfillment of the Requirements
for the Degree of Master of Science

Approved:

Dr. Davin Wallace, Committee Chair
Assistant Professor, Ocean Science and Technology

Dr. Maarten Buijsman, Committee Member
Assistant Professor, Ocean Science and Technology

Dr. Troy Pierce, Committee Member
Chief Scientist, Environmental Protection Agency, Gulf of Mexico Program

Dr. Karen S. Coats
Dean of the Graduate School

December 2016

COPYRIGHT BY

Eve Rettew Eisemann

2016

Published by the Graduate School



ABSTRACT

MODERN FAIR-WEATHER AND STORM SEDIMENT TRANSPORT AROUND SHIP ISLAND, MISSISSIPPI: IMPLICATIONS FOR COASTAL HABITATS AND RESTORATION EFFORTS

by Eve Rettew Eisemann

December 2016

The Mississippi – Alabama barrier island chain is experiencing accelerated sea level rise, decreased sediment supply, and frequent hurricane impacts. These three factors drive unprecedented rates of morphology change and ecosystem reduction. All islands in the chain have experienced land loss on the order of hectares per year since records began in the 1840s. In 1969, Hurricane Camille impacted as a Category 5, breaching Ship Island, and significantly reduced viable seagrass habitat. Hurricane Katrina impacted as a Category 3 in 2005, further widening Camille Cut. To better understand the sustainability of these important islands and the ecosystems they support, sediment transport dynamics must be quantified. In this study, four LiDAR datasets are used to investigate both subaerial and subaqueous volume changes during the most recent intense storm impact, Katrina, and the fair-weather period following. During the Katrina event, sediment comparable to 1.5 times the 2004 subaerial island volume was lost from the topo/bathy system. Only 1/5 of this volume was recovered between 2007 and 2010. The island returned to a net sediment loss between 2010 and 2012, although island area continued to increase. This highlights the importance of full topo/bathy datasets for morphodynamic analyses of barrier island systems. Seagrass patches around the island are primarily limited by exposure to wave energy, but are also limited by depth and rapid deposition

events. Area and volume trends indicate seagrass habitat will not naturally increase, but a Camille Cut restoration may increase habitable area for seagrass if overwash processes are limited.

ACKNOWLEDGMENTS

I would like to first thank my adviser, Dr. Wallace, and committee members, Dr. Pierce and Dr. Buijsman. They provided invaluable guidance as I progressed on my project and wrote this thesis.

I would also like to acknowledge the organizations and people who provided funding, field, and data support for this project. The Mississippi Coastal Improvements Program is the primary funding source. This program involves several agencies including the Environmental Protection Agency (EPA) and the United States Geological Survey (USGS). Data was supplied to me by the Joint Airborne LiDAR Bathymetry Technical Center of Expertise (JALBTCX). Jennifer Wozencraft, Charlene Sylvester, and Celeste Rose of JALBTCX gave me access to LiDAR data and supported me as I learned how to work with it. Crucial fieldwork support was provided by students in the Hydrographic Science program here at USM, Greg Steyer and Darrell Wilson of the USGS, John Anderson of the Gulf Coast Research Lab (GCRL), and Tim Thibaut of Barry A. Vittor & Associates.

Others who supported this project and provided important guidance include Admiral Ken Barbour of USM Hydrographic Science, Dr. Greg Carter at USM Gulf Coast, and GCRL Professor Emeritus, Dr. Ervin Otvos.

DEDICATION

This thesis is dedicated to my parents, Tom & Carol. They gave me the gift of curiosity and the freedom to follow my passion for science.

TABLE OF CONTENTS

ABSTRACT ii

ACKNOWLEDGMENTS iv

DEDICATION v

LIST OF TABLES ix

LIST OF ILLUSTRATIONS x

LIST OF ABBREVIATIONS xi

CHAPTER I – SEDIMENT TRANSPORT AND GEOMORPHOLOGICAL CHANGES
ON SHIP ISLAND, MS 2004-2012 1

 Introduction..... 1

 Geologic Setting..... 2

 Controls on Barrier Island Geomorphology 4

 Sea-Level Rise. 4

 Storm Impacts. 5

 Sediment Supply. 7

 Study Goals..... 9

 Methods..... 9

 LiDAR Data 9

 Digital Elevation Model Creation..... 11

 Digital Elevation Model Analysis..... 12

Errors.....	13
Results.....	14
Digital Elevation Models	14
Island Transects	20
Topo/bathy Volumes and Areas.....	24
Discussion.....	27
Storm Period	27
Fair-weather Period.....	31
Summary	34
Ravinement	34
Aerial and Volumetric Changes.....	35
Conclusions.....	36
 CHAPTER II – RELATING SEAGRASS HABITAT TO EROSION/DEPOSITION	
PATTERNS AROUND SHIP ISLAND, MS	38
Introduction.....	38
Setting	38
Seagrass Background.....	39
Motivation.....	40
Methods.....	41
SAV Surveys.....	41

Sediment Samples	43
Turbidity	44
Analysis.....	44
Results.....	45
SAV Distribution	45
Seagrass.....	45
Macroalgae and Bryozoans.....	46
Grainsize	46
Bathymetry and Bathymetric Change.....	47
Discussion.....	48
Bathymetry.....	48
Erosion/Deposition Patterns.....	50
Exposure to Waves	50
Algae	51
Projected Effectiveness of Camille Cut Restoration.....	51
Conclusions.....	54
REFERENCES	55

LIST OF TABLES

Table 1 Hurricanes and tropical storms	6
Table 2 LiDAR Datasets.....	10
Table 3 Shoreline Retreat Rates.....	25
Table 4 Topographic Data	27
Table 5 Bathymetric Data	28
Table 6 Area and Volume Changes	28
Table 7 Grainsize Data.....	47
Table 8 Seagrass Patch Areas and Elevations.....	49

LIST OF ILLUSTRATIONS

Figure 1. Study Area..... 3

Figure 2. LiDAR dataset elevation distributions..... 11

Figure 3. Conceptual model of the difference calculation. 13

Figure 4. Fort Massachusetts comparison transect: 2004 and 2010..... 14

Figure 5. Gridded LiDAR DEM’s..... 17

Figure 6. Difference grids..... 19

Figure 7. Transect locations. 21

Figure 8. Transects A and B..... 22

Figure 9. Transects C, D, and E..... 23

Figure 10. Shoreline retreat rates..... 24

Figure 11. Transect F..... 25

Figure 12. Island areas, subaerial and subaqueous volumes. 26

Figure 13. Topographic and bathymetric volume changes. 29

Figure 14. Camille Cut channel locations. 30

Figure 15. Ship Island aerial extent over time..... 31

Figure 16. Storm and fair-weather equilibrium profiles..... 35

Figure 17. 2010 and 2014 SAV polygons. 42

Figure 18. SAV polygon detail..... 43

Figure 19. Sediment grab sample locations..... 44

Figure 20. Seagrass polygons. 46

Figure 21. Grainsize contours on topo/bathy DEM..... 48

Figure 22. Patch elevations..... 51

LIST OF ABBREVIATIONS

<i>DEM</i>	Digital Elevation Model
<i>DOC</i>	Depth of Closure
<i>JALBTCX</i>	Joint Airborne LiDAR Bathymetry Technical Center of Expertise
<i>LiDAR</i>	Light Detection and Ranging
<i>LISST</i>	Laser In-Situ Scattering Transmissometry
<i>MHW</i>	Mean High Water
<i>NAVD 88</i>	North American Vertical Datum 1988
<i>NDBC</i>	National Data Buoy Center
<i>NOAA</i>	National Oceanographic and Atmospheric Administration
<i>SLR</i>	Sea-Level Rise
<i>USACE</i>	United States Army Corps of Engineers

CHAPTER I – SEDIMENT TRANSPORT AND GEOMORPHOLOGICAL
CHANGES ON SHIP ISLAND, MS 2004-2012

Introduction

The three major influencing factors on barrier island sustainability are sea-level rise (SLR), storm impacts, and sediment supply. Barrier evolution is governed by a complex balance between these three elements (Byrnes et al., 2013; McBride & Byrnes, 1997; Otvos & Carter, 2013; Twichell et al., 2013). Sea-level rise alone is causing many of the world's sandy coastlines to erode dramatically (Bird, 1985, 1996; FitzGerald et al., 2008). If any of these factors fall further out of balance, a barrier may become unstable and approach runaway transgression (FitzGerald et al., 2006). Documentation exists for unprecedented erosion of Gulf coast barrier systems associated with accelerated sea-level rise punctuated by storm impacts relative to geologic timescales (Anderson et al., 2010, 2014; Wallace and Anderson, 2013). The northern Gulf of Mexico margin is currently one of the most vulnerable sections of coastline in the United States (Pendleton et al., 2010). Over shorter timescales, sediment redistribution along the Mississippi/Alabama barrier chain is controlled primarily by fair-weather, long-shore processes and sediment removal from the system occurs largely due to storms (Byrnes et al., 2013; Otvos & Carter, 2008; Twichell et al., 2013).

These large scale processes at play in barrier systems, and the current state of SLR, storms, and sediment budgets are fairly well understood for this section of the Gulf of Mexico, however few field-based studies quantitatively examine spatial and temporal trends of barrier island evolution (Byrnes et al., 2012; Otvos & Carter, 2008, 2013; Walstra et al., 2012). Modern studies tend to focus on sediment volume changes only

below water level, and area changes on subaerial (above MHW) portions of islands (Byrnes et al., 2012; Morton, 2008; Walstra et al., 2012). The current state of knowledge renders it difficult to describe short term topo/bathy geomorphic processes particularly before and after storm events. Here we aim to quantify both subaerial and subaqueous sediment volume changes on a particularly vulnerable and dynamic island along the Mississippi/Alabama barrier chain, Ship Island, in order to understand geomorphic evolution associated with barrier island change forcing mechanisms.

Geologic Setting

Located along the Mississippi coast, Ship Island is a part of the MS-AL barrier island chain (Figure 1). Ship Island is a part of the Gulf Islands National Seashore. Only a few man-made structures exist on West Ship Island, including the historic Fort Massachusetts, built in the 1860's. Based on heavy mineral provenance (Otvos, 1978), eastern (Appalachian) and western (Mississippi Delta) sources demonstrate the importance of shore-parallel sediment delivery for barrier-shoal construction (Otvos, 2005). Progradational features of the west Mississippi islands reflect this process (Otvos & Giardino, 2004). Based on OSL ages, the western Mississippi barrier islands are documented to be active between ca. 4.6 and 3.7 ka (Otvos & Giardino, 2004), and the adjacent 42-km long New Orleans (Pine Island) barrier-shoal complex (Saucier, 1963, 1994) conforms with these ages (Saucier, 1963; Otvos, 1978; Stapor and Stone, 2004). The barriers stabilized at a relative SLR rate less than 2 mm/yr (González & Törnqvist, 2009; Otvos, 2004; Törnqvist et al., 2004; Törnqvist et al., 2006), in contrast to local or Gulf-wide regression (Otvos, 2005). Modern relative SLR rates in the area of Ship Island

are 4.10 ± 0.92 mm/yr (NOAA Bay St. Louis/Waveland Buoy), averaged between 1978 and 2015, approximately double the rate at which the barriers stabilized.

Barrier sands overlie early Holocene muds that lie ~8 m below the subaerial portion of Ship Island, and extend out ~3 km beyond the shoreline. Barrier sands are onlapped partially by St. Bernard prodelta muds at their most shoreward edge, and shoreface sands are currently topped by a modern erosional unconformity (Twichell et al., 2013).

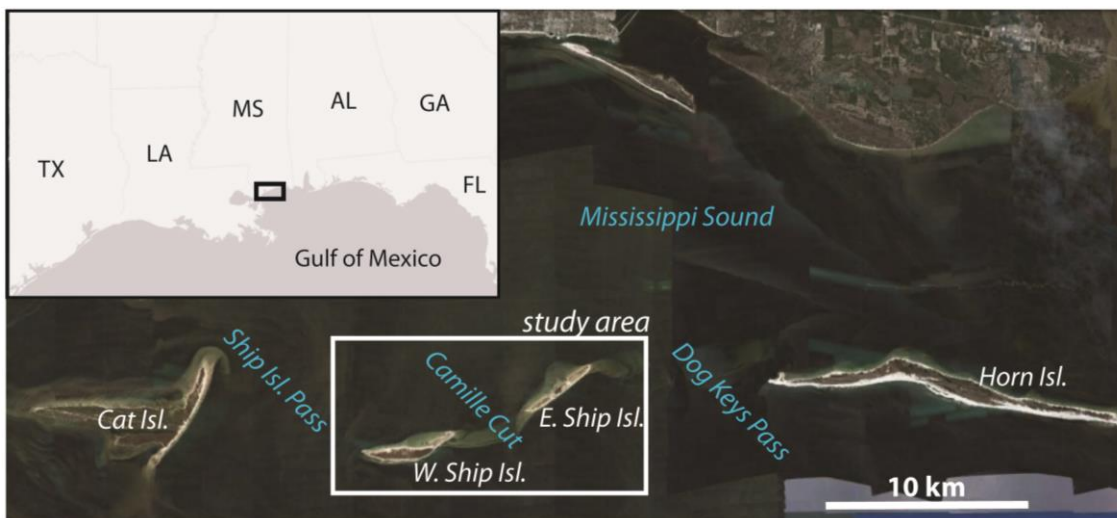


Figure 1. Study Area.

The Mississippi-Alabama barrier island chain is located in the Northern Gulf of Mexico. East and West Ship Islands are shown here in relation to surrounding inlets and the two adjacent islands.

Significant wave height influencing the barrier chain is low with an average of 0.7 m in the winter and 0.4 m in the summer (NDBC – Buoy 42007). The depth of closure (DOC) for the area is ~7 meters, calculated using USACE Wave Information Studies data over the past 33 years (Brutsché et al., 2014). This depth of closure value is verified geologically by the presence of modern muds onlapping the barrier sands (i.e., shoreface toe) beginning at a depth of 8-10 meters on the shoreface. The islands also experience

relatively low tidal energy, with a mean tidal range of 0.45 m and a diurnal range of 0.49 m (NOAA tide gauge 8744756).

The region is frequently impacted by hurricanes and other storms, with 13 tropical storms passing within 100 km of Ship Island since 1960 (NOAA Historical Hurricane Tracks). Hurricane impacts occur here approximately every 10-12 years (Byrnes et al., 2012). The two most intense recorded events, hurricanes Camille and Katrina, impacted the island directly in 1969 and 2005, respectively. Hurricane Camille made landfall as a category-5 in August of 1969, forming the inlet that remains today as Camille Cut. Camille's eye made landfall 45 km to the west of Ship Island (NOAA Historical Hurricane Tracks). Camille brought sustained winds of 160 km/hr to the Gulfport area and a surge of 4.3 meters to Ship Island (USACE, 1970). Katrina impacted approximately 65 km to the west of Ship Island as a strong category-3 hurricane with sustained winds of 200 km/hr and a surge of 8 m on Ship Island (Fritz et al., 2007; Waple, 2005). Geomorphological responses to these events are recorded as the island has been topographically and bathymetrically mapped once before and several times after the Katrina impact using Light Detection and Ranging (LiDAR).

Controls on Barrier Island Geomorphology

Sea-Level Rise. SLR is an important factor of barrier island land loss and disappearance, particularly when considering geologic timescales (Bird, 1985, 1996; FitzGerald, et al., 2006, 2008). An acceleration of SLR or a rate of rise that is faster than the barriers can keep pace with can result in runaway transgression and eventual drowning (FitzGerald et al., 2008; Anderson et al., 2010, 2014). Considering the relative SLR rate at which Ship Island stabilized (~2 mm/yr), and the current relative SLR rate,

(4.1 mm/yr), the system is currently in a state of adjustment and disequilibrium. By the end of this century, both the magnitude and rate of eustatic rise is expected to increase by two to three times (Thomas et al., 2004; Church & White, 2006; Overpeck et al., 2006; Pfeffer et al., 2008; Church et al., 2013).

Healthy barrier island systems respond to SLR in a way that conserves their mass as they migrate landward (FitzGerald, et al., 2008). This is made possible, in part, by the presence of a back-barrier marsh. Marshes reduce water velocity, and consequently erosion on the back barrier. They also provide a foundation for the barrier to transgress upon and reduce tidal prism moving through the inlets (FitzGerald, et al., 2008). However, no fringing marshes currently exist on Ship Island.

The lack of a low energy wetland behind the MS-AL islands, and the large, relatively deep open water of the Mississippi Sound makes Ship Island vulnerable to erosion. Both the shoreface and backbarrier are exposed to high energy waves, and the barrier chain experiences an essentially infinite tidal prism. The chain is therefore highly fragmented, and tidal deltas sequester much of the sediment in the system (FitzGerald, et al., 2008). Rather than conserving mass as they transgress, the MS-AL barriers continuously narrow as they move landward in response to SLR (Morton, 2008).

Storm Impacts. Storm impacts cause dramatic geomorphologic changes along MS/AL barrier island systems over short timescales (days to years) (Otvos & Carter, 2008). Increases in storm frequency or strength could remove more sediment to the back barrier area via overwash and breaching than can be replaced by fair weather processes in a given period, and the island will become increasingly segmented before disappearance (FitzGerald et al., 2008; Sallenger, 2000). Ship Island has been periodically breached

during storms along its vulnerable, low-lying central section (i.e. barrier neck), with the first recorded occurrence in 1852 (Morton, 2008; Otvos & Carter, 2008). East and West Ship Island have been separated and re-unified several times since then by natural island-healing processes (Otvos & Carter, 2008). This was possible with sufficient longshore sediment supply for natural spit growth and eventual island healing between storm impacts (Byrnes et al., 2012; Otvos & Carter, 2008) (Table 1).

Table 1

Hurricanes and tropical storms

Year	Storm	Rating
1960	Ethel	TS
1969	Camille	H5
1979	Fredrick	H4
1985	Elena	H3
1985	Juan	TS
1988	Beryl	TS
1997	Danny	H1
1998	Georges	H2
2002	Hanna	TS
2005	Cindy	TS
2005	Katrina	H3
2009	Ida	TS

Hurricanes and tropical storms chronologically listed passing within 100 km of Ship Island. Data is from the NOAA National Hurricane Center.

In the past century the region has been frequently impacted by hurricanes and tropical storms (Table 1), but Camille and Katrina caused the most significant and lasting geomorphic changes on Ship Island. Katrina significantly expanded Camille Cut, almost completely eroding away the low elevation portion of East Ship, and caused severe shoreline erosion in other parts of the island (Fritz et al., 2007; Morton, 2008).

Significant sediment redistribution can also occur due to cold front storms passing through the area. These systems can produce strong northerly winds and high enough wave energy to erode the back-barrier beaches (Stone et al., 2004). In some cases, these events can be more erosive, particularly in an environment with a large back-barrier fetch like the MS-AL barriers (Byrnes et al., 2012; Otvos & Carter, 2008).

Sediment Supply. A healthy barrier island will be balanced in a dynamic equilibrium of erosion and deposition. Relative decreases in sediment supply can leave an island in a state of net sediment loss, resulting in decreasing size and possible drowning (Byrnes et al., 2013). The primarily quartz sand islands are supplied by beaches, riverine sources, and offshore sands to the east (Otvos and Giardino, 2004). Prevailing easterly winds drive long-shore transport in the region, moving sediment westward along the chain. This is reflected in the general east to west movement and migration of the islands (Byrnes et al., 2012). Despite the seemingly large subaqueous volume of sand supplied to the chain each year (305,000 m³), there is still a net loss of sediment (Byrnes et al., 2013). In fact, Ship Island represents the segment with the largest sediment deficit in the chain at -174,000 m³ per year averaged from 1917 to 2005 (Byrnes et al., 2013). This makes it difficult for the barrier to grow or recover after large erosive events, and contributes to

the reason Ship Island has a relatively small volume above sea level for its length when compared with healthier Florida barriers (Twichell et al., 2013).

More updrift erosion than downdrift deposition is occurring, along with island narrowing and segmentation (Morton, 2008). All MS-AL barriers are in a transgressive/erosional state with occasional progradational/depositional landforms such as spits. This transgression is primarily fueled by movement of sediment to the back barrier via storm overwash, or sediment removal to the deep Gulf of Mexico by storm waves (Otvos & Carter, 2013). Natural island healing after these events is driven by the fair-weather wave sediment supply. In these conditions, shore-parallel bars form in the near shore on the shallow platforms (Otvos & Carter, 2008).

Sediment loss from the system can also be attributed to ship channel dredging (Morton, 2008; Otvos & Carter, 2008). Dredging removes approximately 120,000 m³/yr of sediment from the littoral zone (Byrnes et al., 2012). This decreases the natural long-shore transport supply and deepens the channels from natural depths of around 4.5-5.7 meters to up to 20 m in the Gulfport Ship Channel directly west of Ship Island (Morton, 2008). This leaves sediments in the channels far below fair weather wave base, and functionally isolates one barrier from the next, as evidenced by the lack of sand transport between Ship and Cat Islands (Byrnes et al., 2013). Significant area loss is documented for all islands in the MS/AL chain, but Ship Island is the most vulnerable considering it is one of the farthest from the sand source and already shows more degradation than any other barrier in the chain (Byrnes et al., 2013).

Study Goals

Island area trends suggest that Ship Island, along with the rest of the MS-AL barrier chain, is currently out of equilibrium and shrinking at unprecedented rates (Byrnes et al., 2013). Ship Island has experienced a 66% area loss between 1849 and 2005 (Otvos & Carter, 2008). However, a volumetric analysis has yet to be conducted for the combined topo/bathy system. The goals of this study are to quantify this disequilibrium in more detail by observing the short term barrier morphodynamics and provide the most high-resolution geomorphological and sedimentological analysis of the Ship Island system to date. This is accomplished by first examining the immediate response of Ship Island to the Hurricane Katrina impact and the natural recovery period that followed. From this, the relative role of storm conditions and fair weather processes on sediment transport are described and quantified. This analysis aims to shed light towards our understanding of natural barrier island evolution in our current regime of accelerated sea-level rise, frequent intense storm impacts, and limited sediment supply. This information not only informs us of the evolution of Ship Island, but similar barriers globally.

Methods

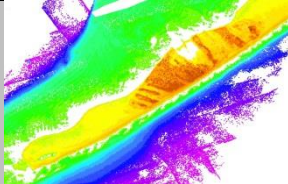
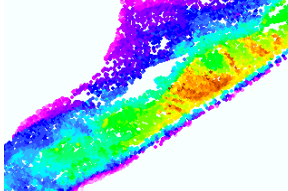
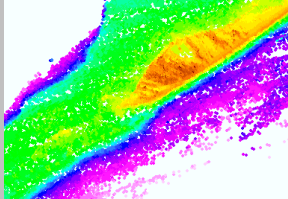
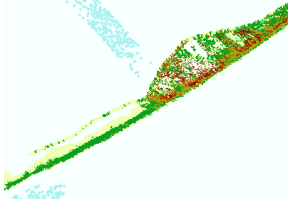
LiDAR Data

LiDAR data were obtained from the Joint Airborne LiDAR Bathymetry Technical Center of Expertise (JALBTCX), located at the Stennis International Airport, MS. Topographic/bathymetric point clouds for 2004, 2007, 2010, and 2012 were available for Ship Island (Table 2). Files were provided in .xyz or .las format and included only the bare earth surface (i.e., vegetation and all other returns were removed). Point clouds were

previewed, clipped to the desired latitude and longitude range, and converted to [x, y, z] ascii files using the LAsTools© (Isenburg, 2015).

Table 2

LiDAR Datasets

Date Collected	Topo	Bathy	Example Segment of East Ship Island	SOURCE	VA 2σ (cm)	HA 2σ (cm)
2012 May	Complete	Complete		USACE NCMP LiDAR Collected by JALBTCX CZMIL system	15 (30 bathy)	100
2010 April	Collected with bathy laser	Complete		USACE NCMP LiDAR Collected by JALBTCX CHARTS system	15	100
2007 June	Complete	Complete		NASA Wallops, USGS Coastal and Marine Geology Program, National Park Service EAARL system	15	100
2004 April	Complete	Limited Coverage		USACE NCMP LiDAR Collected by JALBTCX SHOALS system	~15	100

Sources, dates of collection, data coverage, and errors of the LiDAR datasets used in this study. VA indicates vertical error, and HA indicates horizontal error. These datasets are publicly available from NOAA's online Data Access Viewer.

Once in ascii format, the data were further processed in MATLAB®. Originally referenced to NAVD88, the elevations were converted to mean high water (MHW). Correction values from the NW, NE, SW and SE corners of the study area were obtained from NOAA's VDatum Transformation software. Values were averaged to determine a MHW value on Ship Island of 0.36 ± 0.01 m below NAVD88. Thus, all z values were

converted from NAVD 88 to MHW by subtracting 0.36 m from each. This was done to use a more geomorphologically accurate shoreline for comparison of subaerial and subaqueous features.

Digital Elevation Model Creation

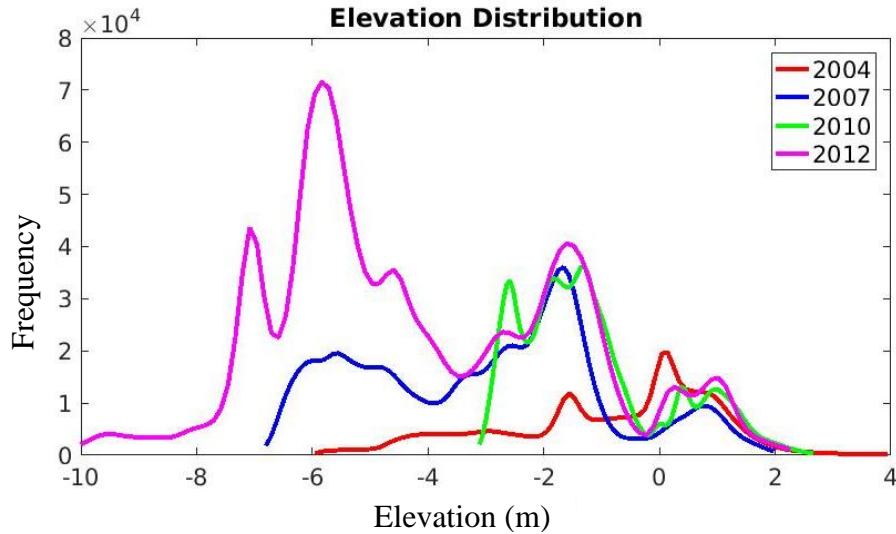


Figure 2. LiDAR dataset elevation distributions.

The frequency at which elevations occur in the four datasets is plotted here, including both topographic and bathymetric data. The data shown here is pre-gridded, so the data is not biased towards areas with denser data coverage.

Each of the [x, y, z] point clouds were gridded to 5 m² cells using a linear interpolation algorithm to create digital elevation models (DEM). The data were gridded within polygons drawn to contain only areas with topo/bathy points. The geographical extent of the data differs from year to year primarily because of water clarity, but also due to instrument limitations and flight line patterns. The geographically smallest dataset used in this study is for the year 2004, which is severely limited in its bathymetric coverage (Table 2). 2010 also contains limited bathymetric data. 2007 and 2012, however, have complete coverage of the shallows around the island, and reach depths up to ~10 m in the 2012 dataset (Figure 2).

Digital Elevation Model Analysis

Analysis of these final DEM's included sediment volume and sediment volume change calculations, and the creation of difference grids using methodologies similar to Buijsman et al., 2003. Sediment volume above MHW, calculated using Equation 1, indicates the sediment volume of the subaerial island:

$$V_{topo} = \iint Z_{aboveMHW} dx dy \quad (1)$$

where V_{topo} is volume (m^3), Z is elevation above MHW for each grid square (m), and $dx dy$ is grid square area ($5 m^2$). Sediment volume below MHW was examined indirectly using the volume of water (Equation 2). In order to compare years with varying bathymetric data extents, the grids are trimmed to the largest area common to all four datasets:

$$V_{water} = \iint Z_{belowMHW} dx dy \quad (2)$$

where V_{water} is volume (m^3), Z is elevation for each grid square (negative below MHW) (m), and $dx dy$ is grid square area ($5 m^2$). Total topo/bathy sediment volume changes are calculated using Equation 3, where ΔV_{topo} and ΔV_{water} are the changes in topographic volume and water volume respectively, from one year to another:

$$\Delta V_{sediment} = \Delta V_{topo} - \Delta V_{water} \quad (3)$$

Difference grids were created from dataset A to dataset B, for example, by subtracting Z values of each grid square in dataset B from the corresponding grid square in dataset A (Figure 3). Difference grids are limited to the area where dataset A and B overlap.

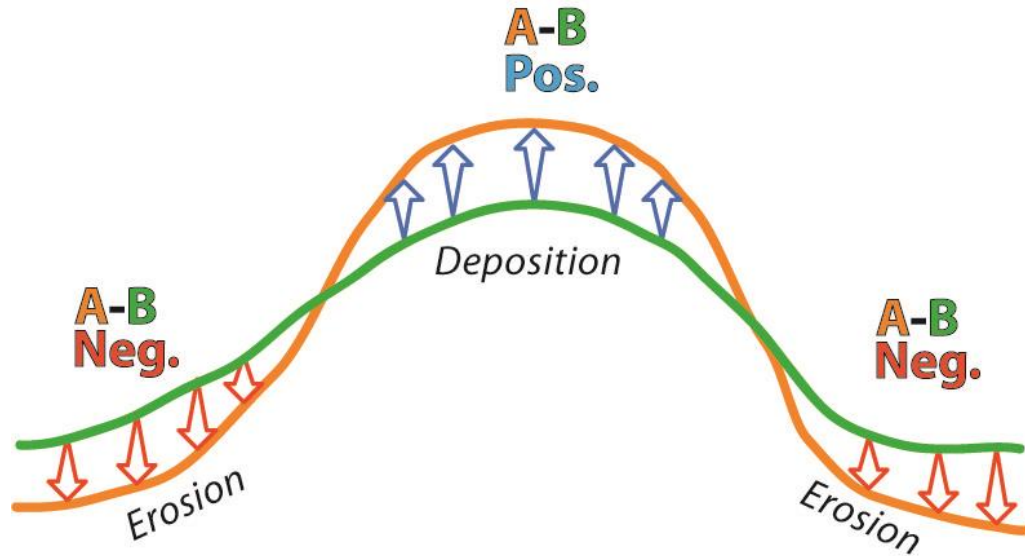


Figure 3. Conceptual model of the difference calculation.

A topographic cross section of the first year (A) is shown in green, and the second year (B) is orange. Subtracting year B from A leaves a positive signature for deposition and a negative signature for erosion.

Cross sectional profiles of East and West Ship Island are created directly from the [x, y, z] point clouds. Transect endpoints are chosen to bisect the islands perpendicular to their Gulf of Mexico shorelines at several representative locations on East and West Ship Island, in addition to across Camille Cut to show changes in the inlet size and depth over the study period. A linear interpolation algorithm calculates values between points along each transect.

Errors

Vertical and horizontal point errors for each LiDAR data point are reported in the metadata for each LiDAR dataset (Table 2). These point errors become negligible when considering the number of points in the datasets. A vertical bias does exist between the datasets, however. This bias is visible in transects across Fort Massachusetts (Figure 4). The elevations on Fort Massachusetts have not remained static over these timescales, as it

has sand deposits and shrubs on its roof. This is clear in the central portion of the transect. The most stable portions are hard structures, such as the brick floor and walkways (Figure 4, Boxes 1&2). The average bias, calculated from differencing transects along these stable portions is 0.23 m. A vertical error envelope of ± 0.12 m is applied to the data and analyses. These errors apply to all DEM's presented here, and are additionally used to calculate maximum area and volume errors. Island area errors are based on the changing island perimeter with the elevation uncertainty. Retreat rate errors were all ~ 2 m based on very similar steepness along the shoreface at each transect location.

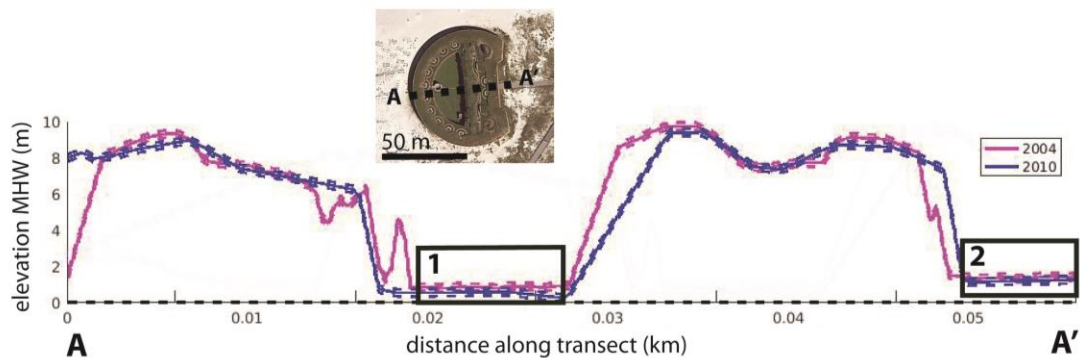


Figure 4. Fort Massachusetts comparison transect: 2004 and 2010.

A comparison of 2004 and 2010 LiDAR data along a transect across Fort Massachusetts (location shown in the satellite image inset). Areas with the best agreement, outlined in the black boxes (1 and 2), correspond with solid portions of the fort devoid of vegetation.

Results

Digital Elevation Models

DEM's were created for 2004, 2007, 2010, and 2012 showing the topo/bathy distribution around Ship Island and the aerial extent at each of these years (Figure 5). Difference grids were created to show elevation changes from 2004 to 2007, 2007 to 2010, and 2010 to 2012 (Figure 6). Basic geomorphological changes are visible in the

DEM's. These changes can be quantified for the three time slices in the difference plots to provide rates of volume change and other valuable metrics (Buijsman et al., 2003).

In 2004, Ship Island has the largest surface area and the smallest inlet relative to the other years. The narrow, low-lying, spit-like feature extending from East Ship Island towards West Ship Island, referred to here as the barrier neck, minimizes Camille Cut to only ~1 km wide (Otvos & Carter, 2008; Figure 6, 2004 to 2007). Most of this neck exists at less than 1 m elevation (Figure 5). The 2004 dataset displays the smallest bathymetric data coverage, so limited information exists concerning the shallow platform around the island at this time. The subtidal section of the beach profile, here referred to as the shoreface, of both East and West Ship drops off quickly to depths of ~5 m on the Gulf side (McBride, et al., 2013).

The first time slice, 2004 to 2007, shows the most erosion of all three difference grids, where the expansive 2004 island area is reduced to what remains in the 2007 DEM (Figure 5). The strongest erosional signatures occur where the low-lying neck existed and along the southern shore lines, where erosion was >1 m/yr (Figure 6). The north shore of West Ship also experienced significant erosion on the order of 0.5 m/yr. The only notable depositional feature in this difference grid exists to the south and west of where the low-lying neck existed before its total erosion. Depositional rates in this area are up to 0.8 m/yr.

The 2007 DEM shows the island with its area reduced by 42%, and volume is reduced by 41% when compared with 2004 (Figure 5). Camille Cut was eroded to nearly 5 km wide. A pond has formed in the central portion of East Ship Island. The eastern tips of both islands are narrower by ~100 m. 2007 data provides complete coverage of the

shallow bathymetry around the island, showing the wide shallow shelves <2 m deep to the north of both islands, and deeper water (~5 m) directly abutting the southern shores. Shoals <2 m deep also extend off the eastern tip of East Ship Island several kilometers into Dog Keys Pass. These eastern shoals, along with the shallow shelves north of the islands appear in all subsequent years where bathymetric data is present, and do not significantly change shape.

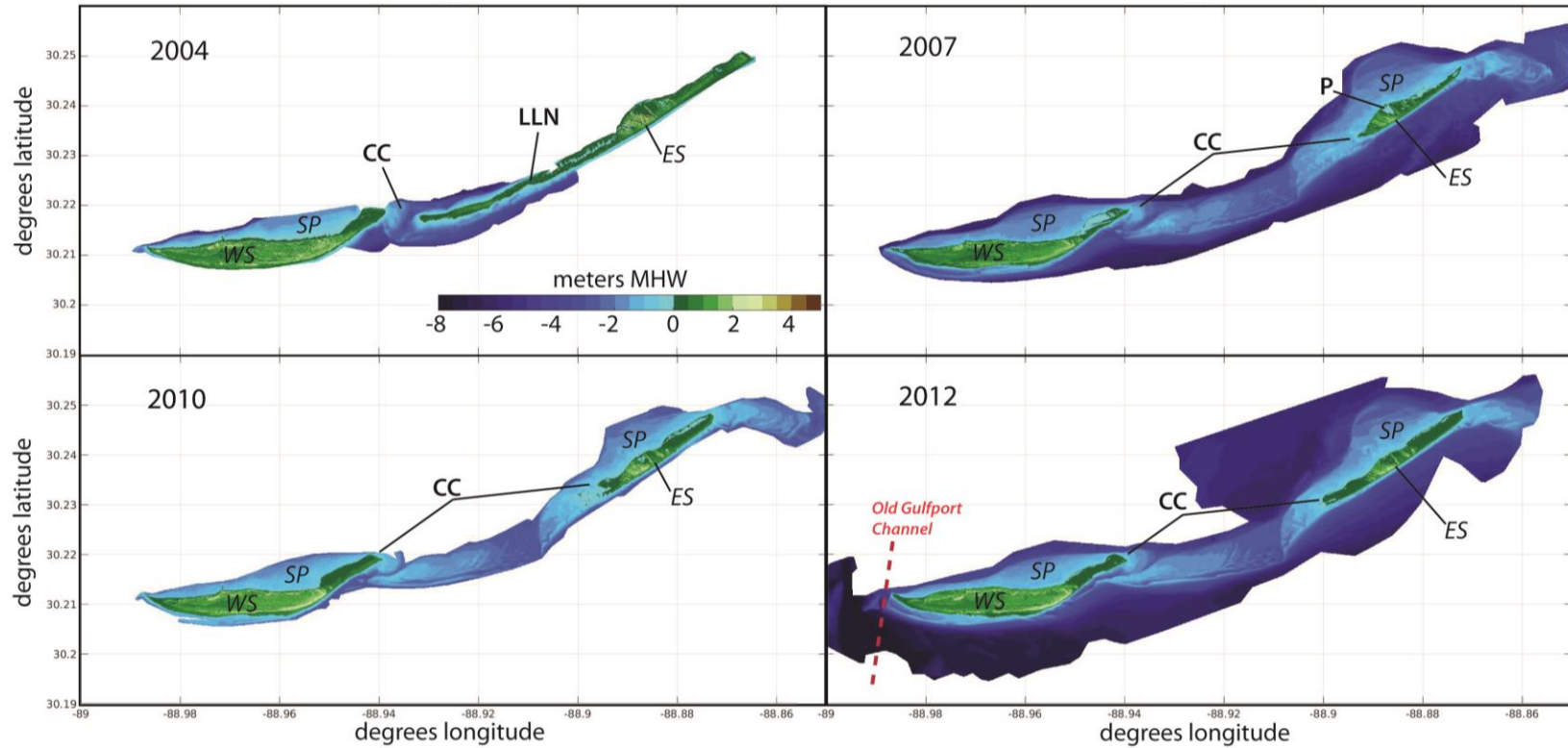


Figure 5. Gridded LiDAR DEM's.

The gridded topo/bathy data DEM's derived from available LiDAR data show elevation and bathymetry for 2004, 2007, 2010, and 2012. The aerial extent of each DEM is limited by LiDAR data coverage. Island topo/bathy is fully visualized, and colored to indicate areas above MHW in green and brown. Features labeled on the DEM's include ES- East Ship Island, WS- West Ship Island, CC – Camille Cut, LLN – Low-lying Neck, SP – Shallow Platform, P- Pond, and the Old Gulfport Channel.

From 2007 to 2010, the difference plot shows significantly more deposition overall, though up to 0.6 m/yr of erosion still exists along the southern shoreface, and the southern edge of the now sub-aqueous portions of East Ship Island (Figure 6). Deposition of 1 m/yr or more occurred in a small patch along the north-west tip of West Ship Island, where the old Gulfport Harbor Navigation Channel (no longer in use) runs (USACE, 2010). The north-eastern tip of West Ship Island shows a larger depositional area up to 0.6 m/yr. Other depositional hot-spots of the same magnitude occur along the edges of the shallow platform, along the western Camille Cut channel, and on both the east and west tips of East Ship Island. The majority of the shallow platform around the island is experiencing negligible change or slight deposition (+0.1-0.2 m/yr).

Between 2007 and 2010, the island increased its area by 15% and its volume by 35%. The net deposition on the island has reduced the size of the inland pond on East Ship. This year reveals in-filling of the previously narrowed eastern island tips to elevations <1 m above MHW, and reappearance of part of the low-lying neck. The two channels in Camille Cut have also evolved, with the eastern channel becoming more linear, and the western channel narrowing.

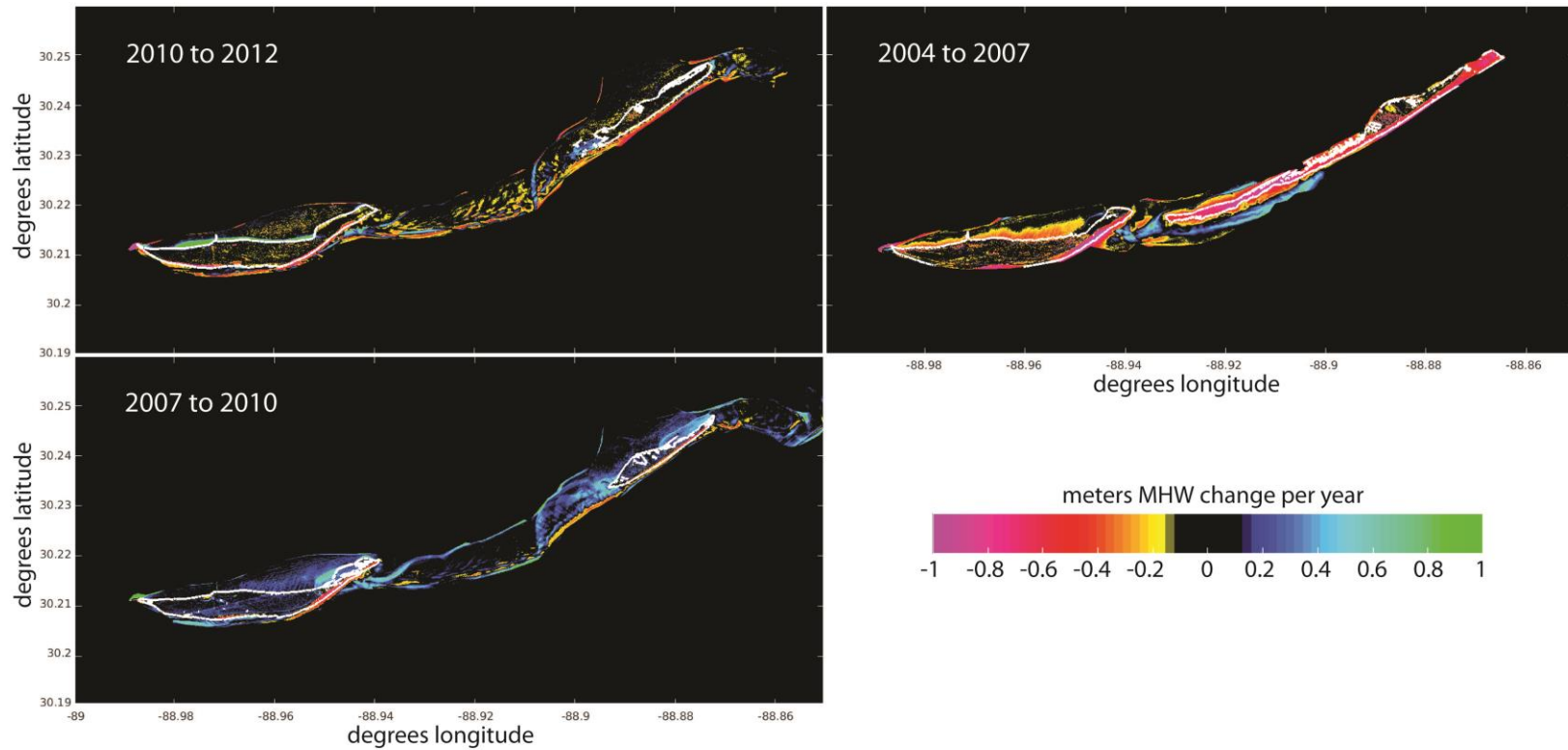


Figure 6. Difference grids.

Difference grids, created by subtracting one Dem year from another, are plotted here with the first year's island outline in white. The color scale indicates erosion in warm colors and deposition in cool colors. Insignificant changes are shown in black.

The 2012 dataset is the most recent detailed topo/bathy data that exists for Ship Island (Figure 5). The bathymetric data coverage is the largest of all four datasets, and shows all the shallow water around the islands as well as deeper portions in Mississippi Sound to the north and the Gulf of Mexico to the south. The western channel of Camille Cut is narrower and curves along the shoreface of West Ship Island. The eastern channel appears relatively stable from 2010 to 2012, however. The 2012 state of the islands shows a slight increase in aerial extent, 8%, but a negligible change in island volume since 2010.

Island Transects

Two transects (A, B) are constructed perpendicular to the Gulf of Mexico shoreline of West Ship Island, three (C, D, E) lie across East Ship Island, and one across Camille Cut (F) (Figure 7). 2004, 2007, 2010, and 2012 profiles were created along each of these transects, and include both subaerial and subaqueous sections. The vertical error for all profiles is ± 0.12 m. One transect was chosen on both East and West Ship to reflect the most stable, high elevation, portions of these islands (Figure 7, transects A and D). These cross areas with the highest elevations and the most vegetation. The other transects cross dynamic portions of the islands. Transects A and D do not show significant elevation change from year to year in the central portion of the islands, but some retreat is visible on the south-facing shorelines.

The narrowing of the eastern tip of West Ship island is reflected in the profiles along transect B (Figure 8). The 2004 profile at this location shows a significantly higher elevation foredune ridge, the first shore-parallel dune ridge inland of the beach (McBride, et al., 2013). In the 2007 profile, the shoreline has stepped back 100 m, and the foredune

ridge has been reduced to approximately half the original elevation. In the 2010 and 2012 profiles along transect B, the shoreline continues to retreat ~40 meters between those two years, and the foredune elevation remains approximately the same (Table 3). An offshore bar at ~ 1 m depth is also visible in these final two profiles (Figure 8).

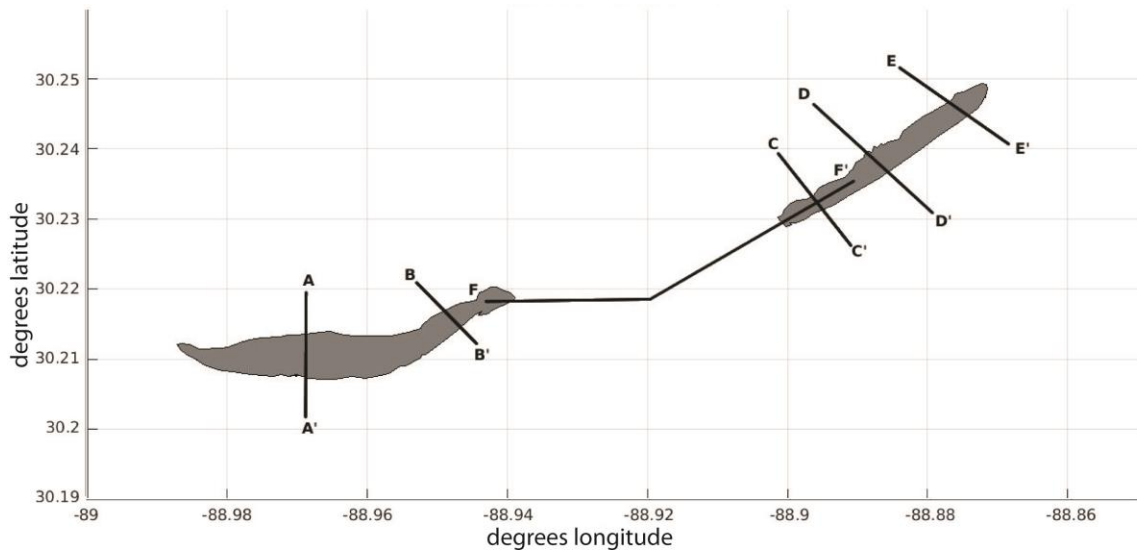


Figure 7. Transect locations.

Two transects are located on West Ship Island, and three are located on East Ship Island. The placement of these transects captures both stable and dynamic parts of the islands. Transect F spans Camille Cut from west to east, showing channel and spit features.

Transects C and E cross the western and eastern tips of East Ship Island respectively (Figure 9). Transect C crosses a portion of the low-lying neck. In 2004 the profile shows a low-elevation (0.5 m) ridge that becomes fully submerged by 2007. The 2007 profile shows a flat, wide, shoal at approximately 2 m depth. The shoal approaches MHW in 2010, and emerges as a subaerial portion of the island again in 2012. An offshore bar is also visible here in 2012 at 0.75 m. Transect E is on the eastern portion of the island, and shows shoreline retreat from 2004 to 2012 similar to that shown along transect B (Table 3, Figure 10). The elevation of the foredune ridge remains

approximately the same through these years. The barrier is narrowed from 200 m to 100 m from 2004 to 2007, followed by widening in 2010 and 2012.

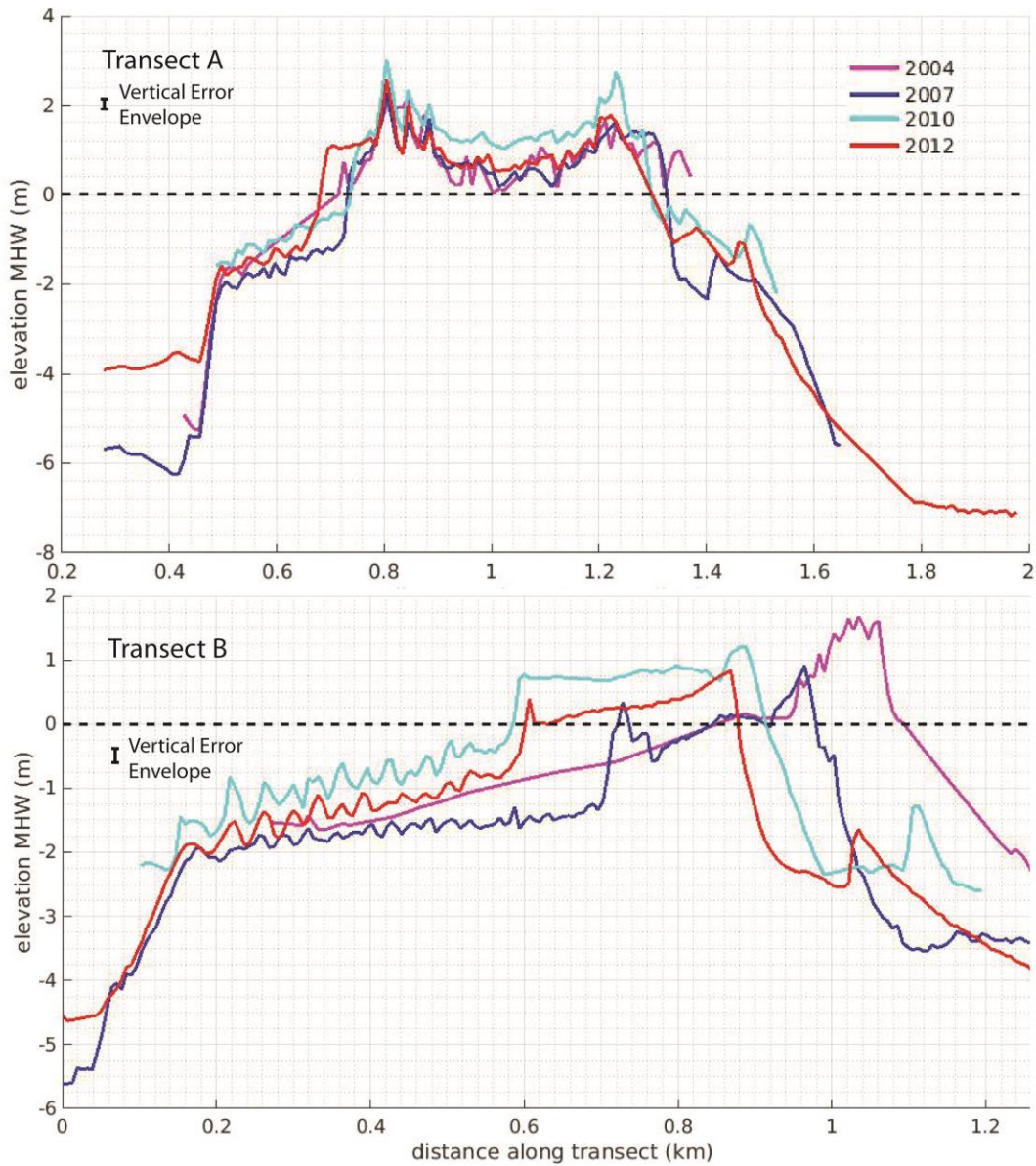


Figure 8. Transects A and B.

Transects A and B are located on West Ship Island, and distance along transect is from north to south (Mississippi Sound to Gulf of Mexico shoreline). Mean high water level is indicated by the dashed line. The error envelope represents the 0.23 m bias.

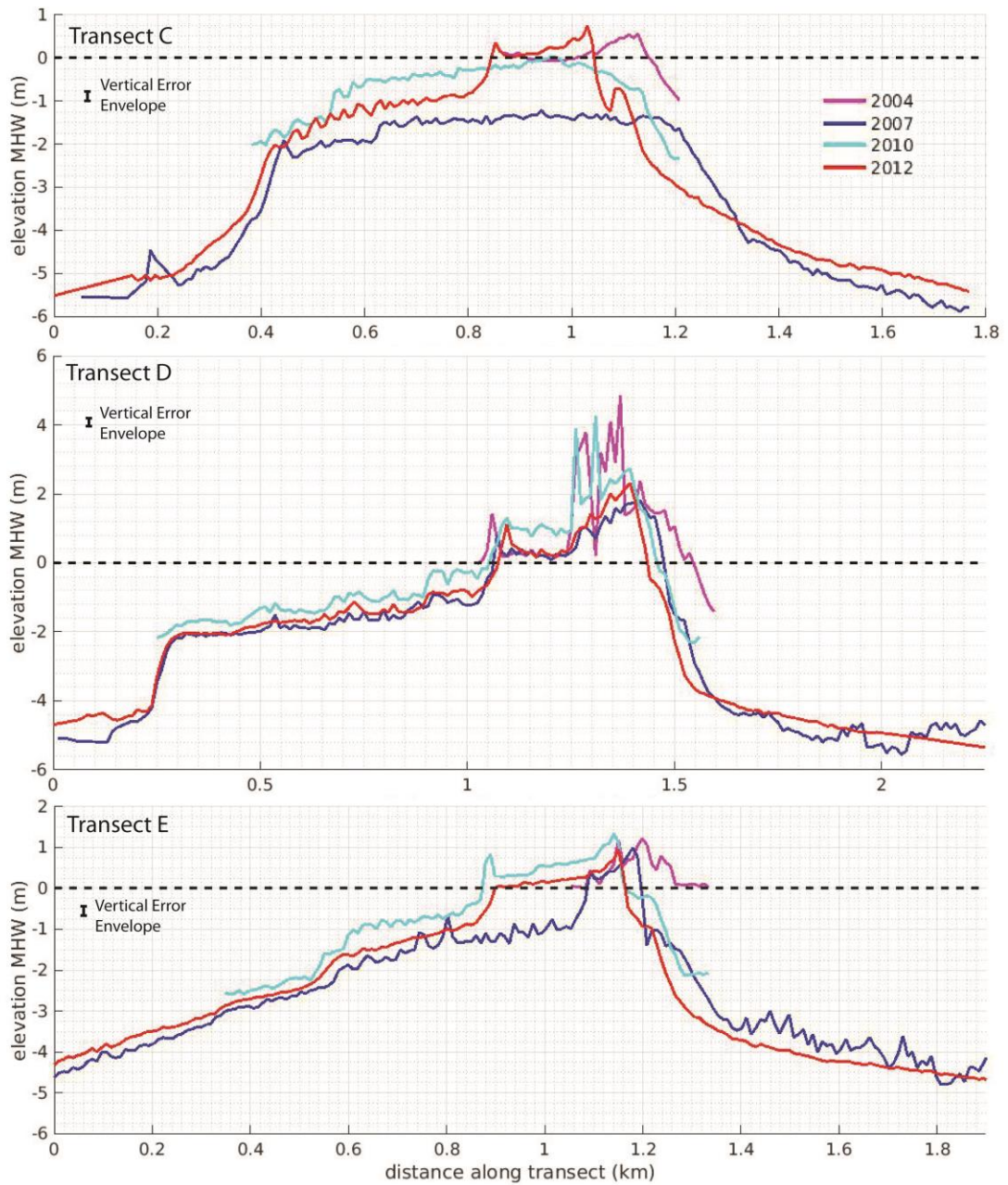


Figure 9. Transects C, D, and E.

Transects C, D and E are located on East Ship Island, and distance along transect is from north to south (Mississippi Sound to Gulf of Mexico shoreline). Mean high water level is indicated by the dashed line. The error envelope represents the 0.23 m bias.

The Camille Cut transect shows the disappearance of the low-lying neck from 2004 to 2007 (Figure 11). Growth along the western tip of East Ship Island appears in the 2010 and 2012 profiles where the eastern part of Camille Cut returns to slightly above

mean water level. The western channel of Camille Cut is present in all four profiles, but shallows from 2007 to 2010/2012 by ~2 m. The Eastern channel reaches its greatest depth, around 4 m, in the most recent profile.

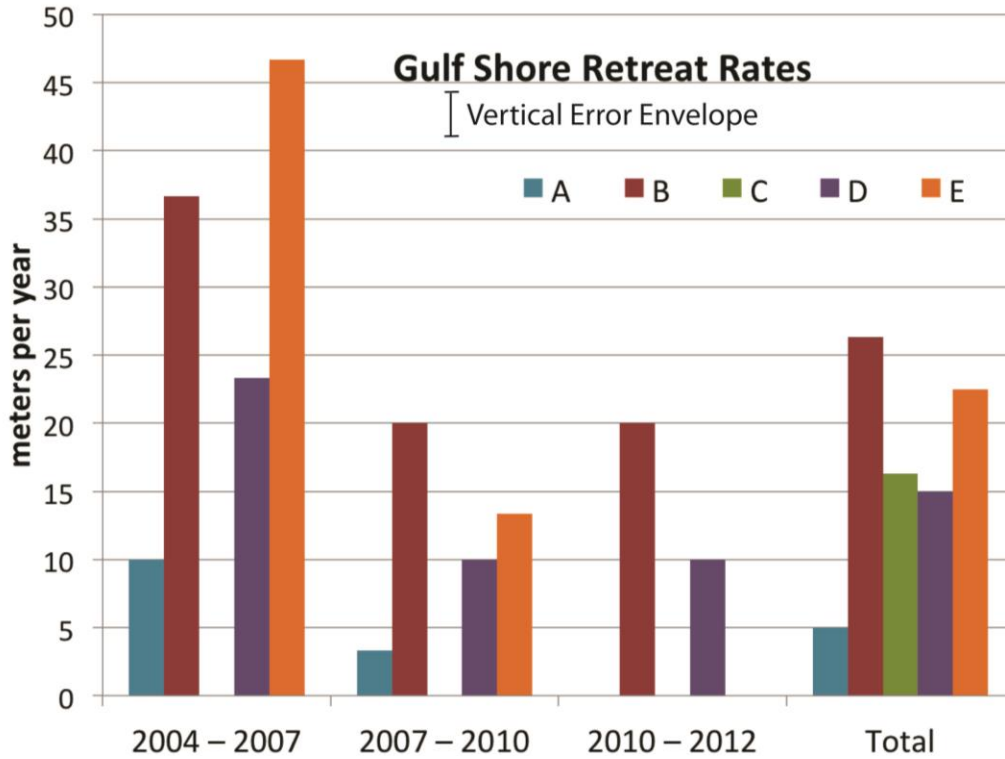


Figure 10. Shoreline retreat rates.

Retreat rates (meters per year) are plotted here for each transect (A-E). Data is shown in Table 3. Total values reflect the average rate of retreat from 2004 to 2012.

Topo/bathy Volumes and Areas

The combined island area in 2004 was 3.90 km², which was reduced to 2.24 km² in 2007 (Table 4). From 2007 to 2010 the island grew to 2.58 km² and again from 2010 to 2012 to 2.80 km². From 2004-2012, the island lost a total of 1.10 km². An increase at an approximately linear rate of 0.12 km²/yr island area is calculated from the LiDAR datasets from 2007-2012.

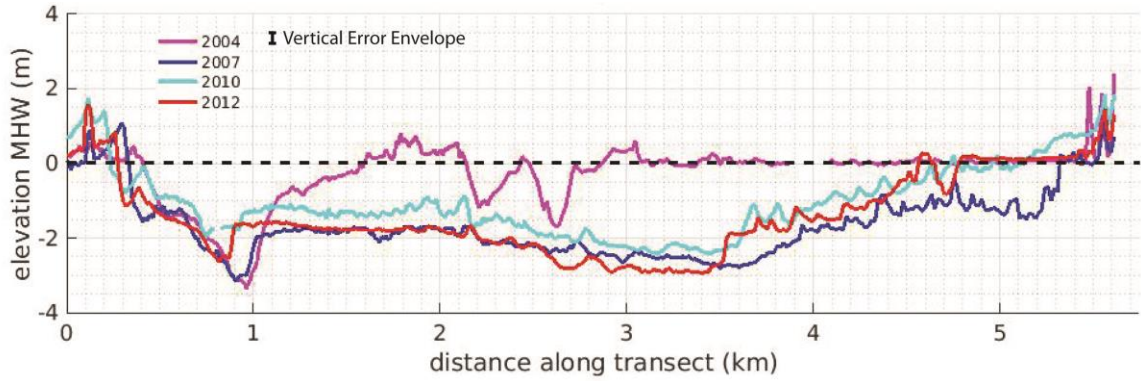


Figure 11. Transect F.

Transect F spans Camille Cut from West to East. Distance along transect is from west to east. Mean high water level is indicated by the dashed line. The error envelope represents the 0.23 m bias.

Table 3

Shoreline Retreat Rates

	A	B	C	D	E
2004 – 2007	30*	110	N/A	70	140
2007 – 2010	10	60	N/A	30	40
2010 – 2012	0	40	N/A	20	0
<i>Total (m)</i>	40	210	130	120	180
<i>Rate (m/yr)</i>	5.0	26.3	16.3	15	22.5

Shoreline retreat rates calculated for transects A-E. All values carry a ± 2 m error. *Estimated value where data does not reach MHW.

Subaerial island volumes as well as bathymetric volumes were calculated from these datasets, and each showed distinct trends throughout the time steps. Island volume decreases drastically, similar to island area, from 2004 to 2007. It is reduced by 1.2×10^6 m³ over this time slice, primarily due to the removal of the low-lying neck and nearshore material. From 2007 to 2010, the island increases its volume by 0.6×10^6 m³. The largest addition of volume in this time slice is back-barrier spit growth and in the old shipping channel (Figure 12). In the final time slice from 2010 to 2012, island volume is reduced

very slightly. The volume increase from 2007 to 2012 is not an approximate linear trend like the observed increase in area.

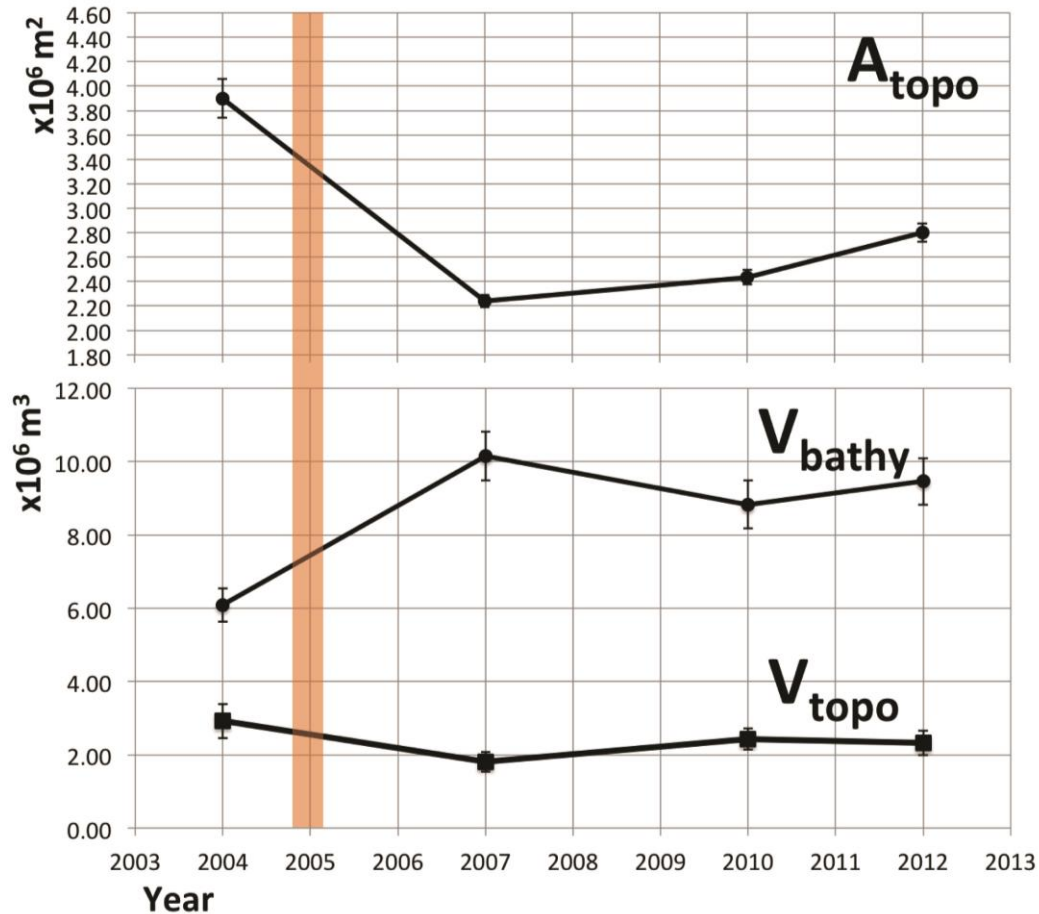


Figure 12. Island areas, subaerial and subaqueous volumes.

Plots of total island area (A_{topo}), subaerial island volume (V_{topo}) and subaqueous island volume (V_{bathy}) show values for the four datasets; 2004, 2007, 2010 and 2012. The Katrina event occurred in 2005 and is indicated here by an orange bar.

Bathymetry changes are observed within the largest data area covered by all four datasets (Figure 13). Water volume increases by $4.1 \times 10^6 \text{ m}^3$ from 2004 to 2007, indicating an overall deepening of the bathymetry around the island (Table 5). From 2007 to 2010, the water volume decreased by $1.3 \times 10^6 \text{ m}^3$, indicating an overall shallowing. In the last time slice, 2010 to 2012, the water volume increases again, but by a small amount, $0.6 \times 10^6 \text{ m}^3$. This trend of deepening via loss of subaqueous sediment,

shallowing due to deposition, and slight deepening again around the islands and in Camille Cut is very similar to the subaerial volume trends observed in the three time slices.

Table 4

Topographic Data

Year	Area (m ²)	Area Error (m ²)	Volume (m ³)	Volume Error (m ³)
2004	3.9x10 ⁶	1.6x10 ⁵	3.0x10 ⁶	4.7x10 ⁵
2007	2.24x10 ⁶	5.0x10 ⁴	1.8x10 ⁶	2.7x10 ⁵
2010	2.58x10 ⁶	5.8 x10 ⁴	2.4x10 ⁶	2.9x10 ⁵
2012	2.80x10 ⁶	7.4 x10 ⁴	2.3x10 ⁶	3.4x10 ⁵

Topographic volume, area, and volume to area ratios for each of the four datasets are presented here. Volume to area ratios indicate the volume of sediment associated with each square meter of island area.

Overall totals reveal the net loss of sediment in the subaerial and subaqueous portions of the island within the data area. The total sediment loss from 2004 to 2007 is $5.2 \times 10^6 \text{ m}^3$ (Table 6). Sediment volume increase from 2007 to 2010 is $1.9 \times 10^6 \text{ m}^3$, and from 2010 to 2012, $0.7 \times 10^6 \text{ m}^3$ was lost from the observed system. The total sediment volume lost since 2004 is a minimum value due to the lack of data coverage for 2004, and larger data coverage in all following years.

Discussion

Storm Period

Erosion and land-loss dominate the stormy period, 2004 to 2007, which captures the Katrina impact of 2005. Katrina’s eye passed 65 km to the west of Ship Island, exposing it to the strongest quadrant of the cyclone. The East Ship neck existed nearly at sea-level, and was easily overtopped completely by Katrina’s storm surge. The storm surge and waves effectively flattened this landform to a wide, subaqueous platform.

Table 5

Bathymetric Data

Year	Volume Water (m ³)	Volume Error (m ³)
2004	6.1x10 ⁶	4.6x10 ⁵
2007	10.2x10 ⁶	6.7x10 ⁵
2010	8.8x10 ⁶	6.5x10 ⁵
2012	9.5x10 ⁶	6.4 x10 ⁵

Bathymetric area, volume, and volume to area ratios for each of the four datasets. Volume to area ratios indicate the volume of water associated with each square meter of bathymetric area. DEM's were all trimmed to the largest common area included in all datasets.

Table 6

Area and Volume Changes

2004 – 2007 (Storm Period)	Sediment Volume Change x10 ⁶ m ³	Island Area Change x10 ⁶ m ²
Bathy	-4.1	
Topo	-1.2	-1.7
Total	-5.3	
2007 – 2010 (Fair-weather Period I)		
Bathy	1.4	
Topo	0.6	0.4
Total	2.0	
2010-2012 (Fair-weather Period II)		
Bathy	-0.7	
Topo	-0.1	0.2
Total	-0.8	
NET CHANGE	-4.1	-1.1
AVE RATE	-500,000 m³/yr	-140,000 m²/yr

Topo/Bathy sediment volume and area changes over each time slice are shown. Net volume and area changes as well as time-averaged rates of volume and area change are calculated. Bathymetric volume bias is approximately 5x10⁵ m³ and topographic volume bias is approximately 3x10⁵ m³. Area error is approximately 1x10⁵ m². Values that are close to the magnitude of the errors are italicized to indicate small or insignificant change.

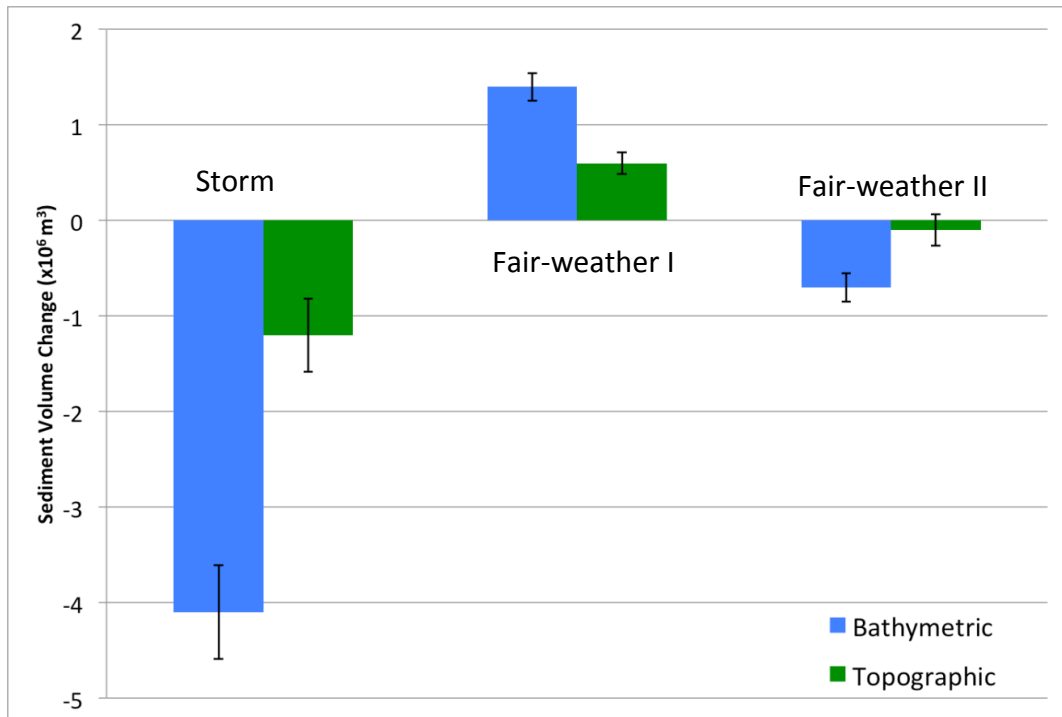


Figure 13. Topographic and bathymetric volume changes.

Total sediment volume changes in the three time slices are shown here. The storm period is 2004-2007, fair-weather I is 2007-2010, and fair-weather II is 2010-2012. Error bars are calculated using ± 0.12 , half the bias, multiplied by the area of the island or bathymetric zone of interest.

This explains the erosive signature of the neck surrounded by a depositional feature in the shallow nearshore and backbarrier. The flattening of the neck to below MHW level increases the width of the inlet by ~5 times. Inlet/channel width increases in response to storm events are documented in other locations along the MS/AL chain during Katrina (Fritz et al., 2007). Some of the material removed from the neck was deposited to the west into the former main channel of Camille Cut. Another channel emerged ~3 km east of the original (Figure 14). This new channel formed at the boundary where a wide platform existed to the east and to the west the back-barrier shoreface drops off relatively

quickly into the deep MS Sound (Figure 14). These subaqueous features are not captured in the LiDAR dataset for 2004, but are visible in satellite imagery from January 2005.

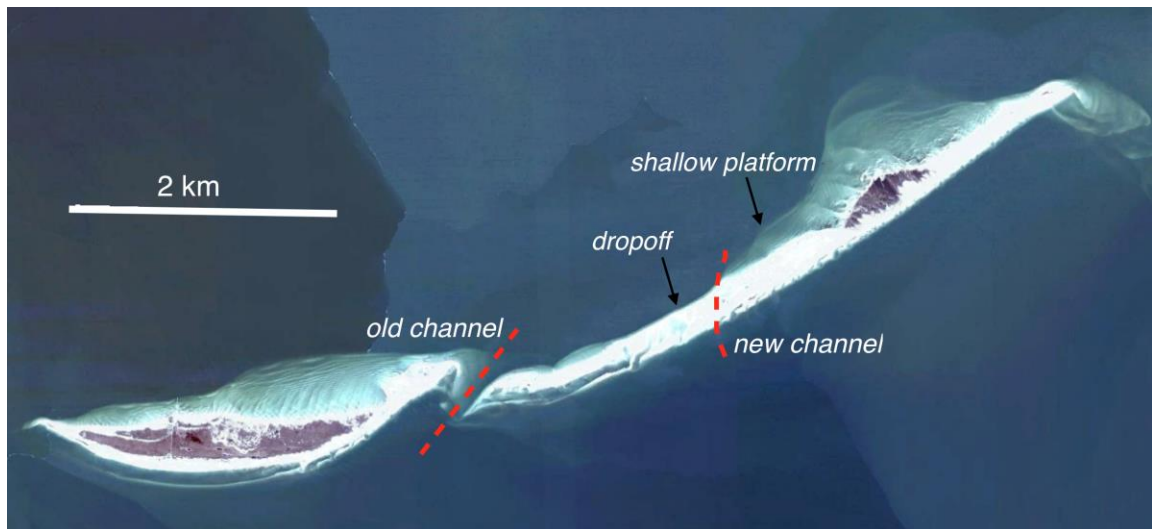


Figure 14. Camille Cut channel locations.

The new and old Camille Cut channels are shown as red dashed lines on a satellite image of Ship Island taken in January 2005, before Katrina. The extent of back-barrier shallow platforms and the relation to the formation of the new channel is visible in the image.

The shorefaces (shallow subaqueous) and beaches of both East and West Ship Island suffered severe erosion during Katrina's impact (Figure 6). The central, most stable, portions of both islands suffered shoreline step-back, 30 m on West Ship, and 70 m on East Ship (Figure 8). Some inundation did occur on these stable portions as well, killing all remaining pine trees and forming a pond on East Ship (Otvos & Carter, 2008). On the eastern tip of West Ship Island, some sediment removed from the shoreface was redeposited in the back-barrier in a spit feature (Figure 6). Wave refraction around the tip into the relatively protected back-barrier likely allowed for this (Ashton & Murray, 2006). This may have also occurred on East Ship, but that area is not within the 2004 data coverage. Similar back-barrier spits do appear on East Ship in later years.

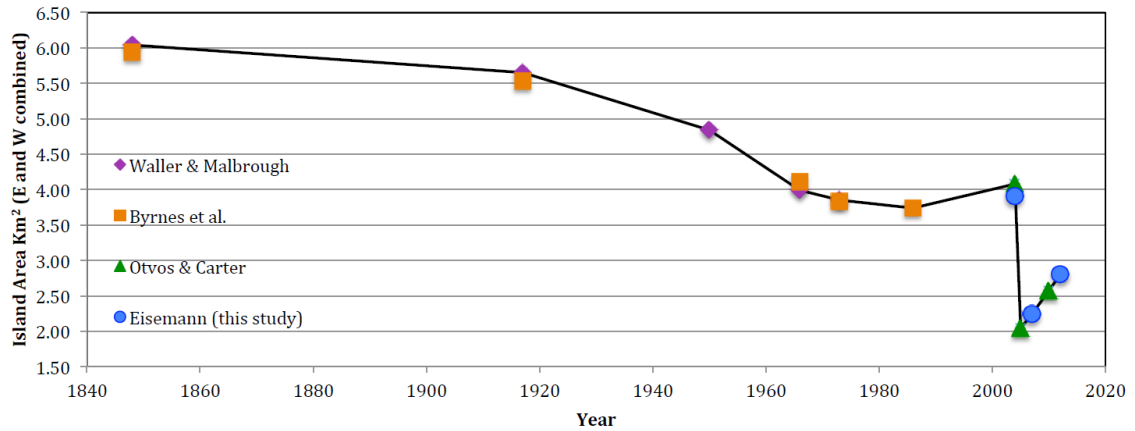


Figure 15. Ship Island aerial extent over time.

Previously published area values (purple diamond: Waller and Malbrough, 1976; Orange square: Byrnes et al., 2013; Green triangle: Otvos and Carter, 2008) for Ship Island are compared with those calculated from the DEM's used in this study.

Not all of the sediment removed from the subaerial island, shallow platform, shorefaces, or the low-lying neck was redeposited in the shallow back-barrier or in Camille Cut. Between 2004 and 2007, the island lost nearly half of its subaerial volume (Table 6). The total topo/bathy system observed in this study lost a minimum of 5.3×10^6 m³ over this period, ~1.5 times the subaerial island volume in 2004. Overwash processes mostly permanently removed a significant amount of sediment from the system. The geomorphological consequences of this sediment removal are visible in the 2007 DEM (Figure 5). The extreme erosion and lack of natural recovery observed in the Ship Island system over this period is similar to the more advanced transgressive state of the Chandeleur Islands in Louisiana (Twichell et al., 2013).

Fair-weather Period

Overwash processes in combination with the lack of new sediment delivery from the east, can explain why only 37% of the sediment volume lost during Katrina was restored before the system returned to a net negative sediment flux (Byrnes et al., 2012).

The little natural recovery can be attributed to the availability of sediments within fair weather wave base in the shallow platform surrounding the island (Otvos & Carter, 2008). High fair-weather wave angle causes continued island step-back, particularly on the eastern island tips (Ashton & Murray, 2006; Morton, 2008). The back-barrier areas all experience deposition, at the expense of this nearshore erosion. Therefore, overwash processes were also slightly constructive along the relatively sheltered back-barrier. Material removed from the eastern shorefaces of the islands is likely supplying the back barrier spit growth, and the widespread but slow accretion in the back barrier shallow platforms.

Between 2007 and 2010, the West Ship nearshore erosional zone experienced $3.2 \times 10^5 \text{ m}^3$ of sediment loss per year. Spit growth in the back-barrier accounted for the deposition of $2.7 \times 10^5 \text{ m}^3$ per year. This value does not include the expansive but slight deposition that occurs across most of the shallow back-barrier platform. During this time slice, East Ship experienced slightly less nearshore erosion, $1.6 \times 10^5 \text{ m}^3$ per year. Erosion slightly offshore is more expansive on East Ship, however (Figure 6, 2007 to 2010). Spit development on the eastern tip of East Ship Island sequestered $2.4 \times 10^5 \text{ m}^3$ of sediment per year, indicating additional sediment sources to the nearshore erosion.

Some material removed from the nearshore remains on the southern side and is transported downdrift. Small depositional features appear parallel to the south-western shorefaces of both islands. One of these features appears as the offshore bar in the 2010 profile along transect A (Figure 8). A considerable amount of the total material eroded from the shoreface is also likely ending up in the old section of the Gulfport Harbor Navigation Channel that lies directly adjacent to the western tip of Ship Island. This same

sediment source, along with erosion along the Gulf side of the eastern Camille Cut shallows, allows the East Ship neck to begin aggrading and extending again.

The new morphology of Camille Cut reduces the velocity at which tidal currents pass through the inlet by increasing its cross-sectional area. As tidal inlets widen and deepen, tidal amplitude typically increases while phase decreases. This is associated with a decrease in frictional force coupled with an increase in celerity (Cai et al., 2012; Chernetsky et al., 2010; Jiang et al., 2012; Zhu et al., 2015). This allows for shoaling in the original western channel, which once accommodated all the water that moves through the cut. The east-to-west longshore currents in the area drives the motion of sediments in the cut, and pushes the channel closer to West Ship Island as it shallows (Figure 11). The newly dominant eastern channel may hinder East Ship Island's ability to naturally extend past this point in Camille Cut.

Some of this eroded material that makes its way onto the subaerial portion of the island is reworked by wind, given these changes are only noted during fair-weather time slices. This suggests that aeolian processes are rebuilding the foredune ridges in a few locations along the islands. The 2010 profiles along transects A, B, D and E show an aggraded foredune ridge relative to 2007 (Figure 8, 9). The island increases in volume and area during this recovery phase, but only recovers a fraction of that lost (Table 5). All of the recovered volume, and most of the recovered area, appears between 2007 and 2010.

The final time slice, 2010 to 2012, shows a system no longer dominated by the storm impact or recovery, but dominated by limited sediment supply. Although still in a fair-weather period, the island is too starved of sediment to continue its recovery. Spit

growth continues along the East Ship neck, but has essentially halted along the eastern tips of the islands. The shallows now show a net erosional signature, and nearshore erosion continues as before. The foredune ridge, and other subaerial portions of the island, begin to deflate as well at rates up to ~ 0.3 m/yr. As sediment sources around the island begin to reach depletion, less material is supplied to the subaerial island despite a relatively constant rate of aeolian removal.

Summary

Several morphological trends are evident across all three time slices. Nearshore erosion, shoreline retreat, and island rotation occur from 2004 to 2012. Both nearshore erosion and shoreline retreat reach their maximum rates during the period of storm impact, but they continue even into the fair-weather phase (Table 3). Both erosion and retreat are most severe along the eastern tips of the islands, causing the observed rotation. Transects B and E cross the eastern tips of West and East Ship Island, respectively (Figures 8, 9). This can be explained by the large incident wave angle, and a lack of sediment supplied by long-shore drift (Ashton & Murray, 2006). This causes increasing sediment loss from west to east, and consequent counter clockwise rotation of the eastern island tips (Morton, 2008).

Ravinement. The island transects reveal how the island profiles respond to the Katrina impact. On centennial to millennial timescales, stormy and fair weather periods influence the equilibrium shoreface profile (Wallace et al., 2010). A pre-storm equilibrium profile is characterized by a steep upper shoreface. This adjusts to stormy periods by shallowing its slope in response to higher wave energy. The sediment removed from the upper shoreface in this process is pulled offshore to the lower shoreface (Figure

16). Although this study examines changes on a year to year timescale, some of these adjustments are already visible. The upper shore face is the steepest in 2004 where the data is available. From 2004 to 2012 the profiles move towards the post-storm profile (Figures 8, 9). On this short timescale, the island continues to adjust to the Katrina impact, and has not yet reached the post-storm equilibrium profile. Barrier island recovery and adjustment is not always immediate, and islands can take years to fully equilibrate (Stone et al., 2004).

Aerial and Volumetric Changes. The aerial extent of Ship Island has been measured many times since the 1800's, primarily by aerial imagery and later by satellite (Figure 15). The overall trend is one of significant land loss from a total area of ~6 km² in the mid 1800's, when it was still unified, to a total area of only ~2 km² by 2005 (Byrnes et al., 1991; Otvos & Carter, 2013; Waller & Malbrough, 1976). Smaller-scale area changes can be observed before and after storm impacts, like Katrina. After 2005, the island area began to increase again (Otvos & Carter, 2013). This increase is verified by the data presented here (Table 6). The overall storm response observed in this study is the response that can be expected by islands within a regime of sediment supply limitation (Priestas & Fagherazzi, 2010; Stone et al., 2004).

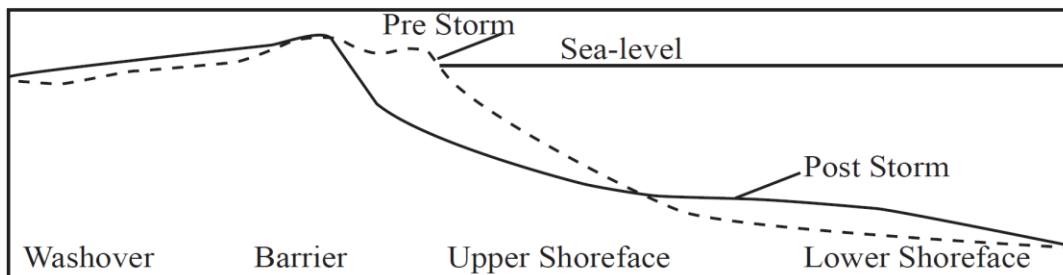


Figure 16. Storm and fair-weather equilibrium profiles.

Equilibrium profiles for stormy and fair-weather periods (modified from Wallace et al., 2010).

Volume change studies conducted on larger temporal and spatial scales can also be compared to values presented here. Byrnes (2013) averages bathymetric changes from 1917/18 to 2005/10 to calculate an overall sediment flux for the entire barrier island chain. Values for each island and for sections of each island are also reported. Ship Island's average bathymetric flux over this time period is $-174,000 \text{ m}^3/\text{yr}$ (Byrnes et al., 2013). The subaqueous sediment flux calculated in this study averaged from 2004 to 2012 is $-430,000 \text{ m}^3/\text{yr}$. When the subaerial sediment flux from this study is included, the value becomes $-500,000 \text{ m}^3/\text{yr}$ from 2004 to 2012. The average rate of sediment loss in the system is more than double when considering the past 10 years compared with the past 100 years.

Conclusions

- I. The island experienced a stormy period from 2004 to 2007 characterized by erosion, followed by a period of fair-weather recovery from 2007 to 2010 and finally stabilization and return to slight net erosion from 2010 to 2012. During the erosional period, a minimum of net sediment loss of $4.1 \times 10^6 \text{ m}^3$ occurred. Ultimately only $\sim 1/5$ of the sediment volume lost during the storm period was recovered during the following fair-weather periods. An average flux of $-500,000 \text{ m}^3/\text{yr}$ occurred across all three periods.
- II. The foreshore and shoreface provided the primary sediment source for areas of growth. This documents typical transgressive barrier island processes.
- III. Natural island volume recovery halted after 2010, though island area continued to increase. This highlights the importance of volumetric versus areal assessments to characterize barrier island geomorphology.

- IV. The system is still equilibrating from Katrina's impact, although with limited sediment supply, could entirely disintegrate (i.e., Chandeleur Islands) during the next major storm impact.

CHAPTER II – RELATING SEAGRASS HABITAT TO EROSION/DEPOSITION PATTERNS AROUND SHIP ISLAND, MS

Introduction

Barrier island systems are ecologically unique. They form the boundary between the high-energy marine environment and low-energy back-barrier marshes, bays or sounds. They are composed of unconsolidated sediments, and are therefore dynamic. Storms, sea-level rise, and sediment supply are the primary controlling factors on their formation, stability, or demise (Byrnes et al., 2013; McBride & Byrnes, 1997; Otvos & Carter, 2013; Twichell et al., 2013). They often provide the most seaward extension of terrestrial and shallow-water ecosystems, and therefore provide habitats to many coastal marine organisms (Handley et al., 2007). One of the most crucial organisms present in these systems is seagrass, a type of submerged aquatic vegetation (SAV), as it provides the base of many of these shallow water ecosystems (Orth et al., 2006).

The northern Gulf of Mexico margin is currently one of the most vulnerable sections of coastline in the United States (Byrnes et al., 2013). Given the recent documentation (Chapter 1) of storm and fair-weather evolution of a particularly dynamic barrier island in the MS/AL chain, Ship Island, this presents a unique opportunity to examine the impact of coastal change on these important SAV habitats.

Setting

The only seagrass species present along Ship Island, and throughout the Mississippi Sound, is *Halodule wrightii* Ascherson, or shoal grass (Carter et al., 2011; Eleuterius, 1987; Handley et al., 2007). Seagrass beds found in the Mississippi Sound lie exclusively on the north side of the barrier islands, and are typically patchy and

discontinuous (Carter et al., 2011; Eleuterius, 1987). This has remained consistent since some of the first documented observations were made in the 1940's (Carter et al., 2011). Many species of shellfish, finfish, crabs, and shrimp present in the Mississippi Sound are known to rely on seagrass ecosystems (Handley et al., 2007). However, these important seagrass ecosystems in the Mississippi Sound, and globally, are in decline (Handley et al., 2007; Orth et al., 2006). In order to best facilitate their recovery in specific locations like Ship Island, Mississippi, the current extent and suitable physical environments for seagrass growth must be examined.

Seagrass Background

Most species of seagrass require shallow, low turbidity and low energy environments so they have sufficient light but are not affected by currents and heavy erosion or deposition (Eleuterius, 1987; Yates et al., 2011). In order for seagrass to colonize and grow, the substratum must be appropriate for rhizomes to establish and fasten. Areas with very mobile substrate conditions, like sediments within the surf zone or in an area of fast currents, are unsuitable (Iverson & Bittaker, 1986). Severe storm impacts can also influence seagrass distributions. The grasses can sometimes be buried or washed away by this type of energetic, episodic event (Eleuterius, 1987). Seagrass patches are capable of withstanding storm impacts if they are sufficiently protected, however (Byron & Heck, 2006; Carter et al., 2011).

In some cases, the presence of seagrass can facilitate sediment deposition and stabilization by slowing bottom currents and fastening the sediments in their roots. This suggests that certain low depositional rates are tolerable for seagrass. Rapid placement of

material thick enough to completely cover the SAV, however, will prevent photosynthesis and kill the plants (Yates et al., 2011).

H. wrightii is found growing in a variety of grain sizes from mud to sand (Iverson & Bittaker, 1986). In coastal Mississippi and Alabama, however, the species is typically found in sandy areas like those surrounding the barriers (Eleuterius, 1987). It has a shallow root system, and often appears early in the successional development of seagrass beds (Dawes, 1987). *H. wrightii* was found to withstand the most exposure during low-tide when compared with other seagrass species growing in Tampa Bay, and was also observed dominating both the deep water and shallow water fringes of multi-species seagrass beds, though its ideal habitat is closer to sea-level (Yates et al., 2011). Along the Mississippi barrier islands, this species of seagrass contributes biomass (~138 g dwt m⁻² on average during optimum conditions) to nearshore environments which are otherwise relatively devoid of organic material (Eleuterius, 1987).

Motivation

The stability of suitable habitat for submerged aquatic vegetation (SAV) in the Mississippi Sound is directly related to barrier island stability (Carter et al., 2011; Eleuterius, 1987). Ship Island, Mississippi has been breached periodically throughout its recorded history (Morton, 2008; Otvos & Carter, 2008). The inlet between East and West Ship Island severely reduces the available seagrass habitat by exposing the back barrier to higher wave and current energy (USACE, 2014). The goal of the MsCIP program is to restore Ship Island to its pre-Camille volume and area.

SAV response to the in-filling of Camille Cut will depend on the sensitivity of this SAV species to shifts in environmental conditions like bathymetry, substrate type,

exposure to waves, deposition and erosion. This investigation will describe the present state of these factors, and the ranges at which *H. wrightii* is currently stable on Ship Island, MS.

Methods

SAV Surveys

Aerial SAV surveys around East and West Ship Island were conducted by Barry A. Vittor & Associates. Two surveys were conducted, one in 2010 (early summer) and 2014 (early fall). Methods employed include aerial imaging and field ground-truthing of locations and SAV type by boat. A detailed description of methods can be found in the Mapping of Submerged Aquatic Vegetation MsCIP Barrier Island Restoration Project Reports, 2011 & 2015. The distributions and types of SAV presented in these reports will be geographically evaluated here to describe the conditions associated with SAV growth and compared with supplementary data such as grain size, bathymetry, and geomorphology.

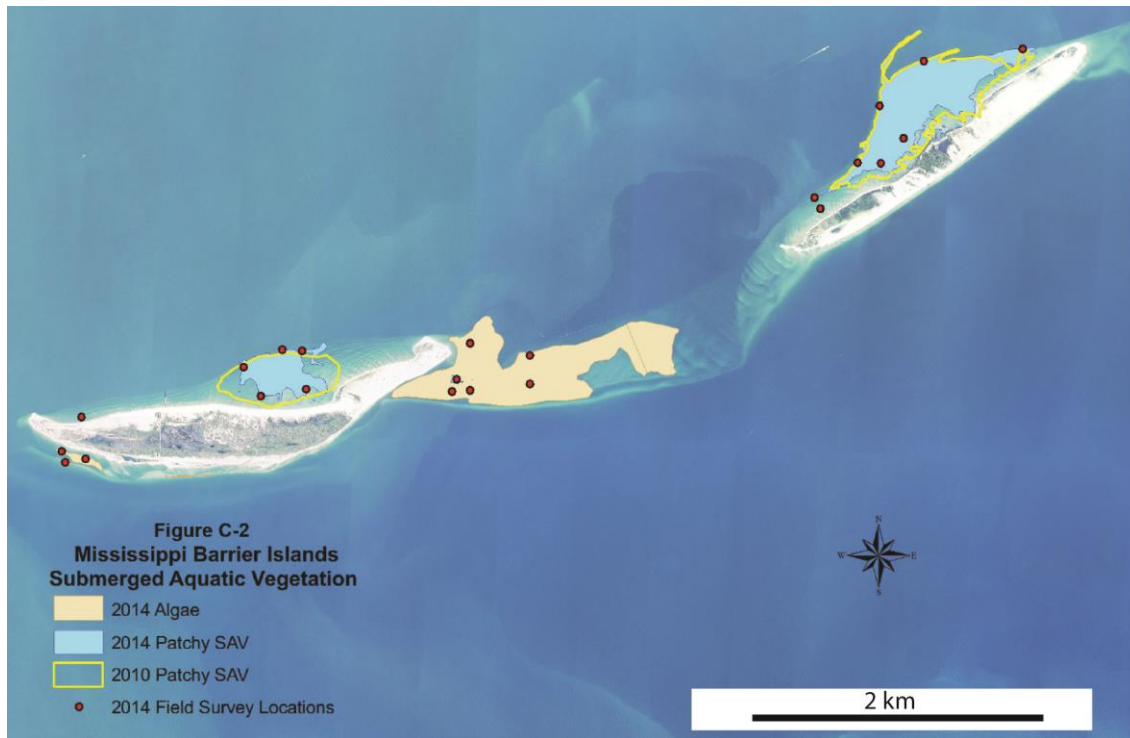


Figure 17. 2010 and 2014 SAV polygons.

SAV polygons from surveys conducted in 2010 and 2014 are shown on a satellite image of Ship Island. Figure modified from Barry A. Vittor & Associates, 2012.

These two surveys were taken during different parts of the growth season to determine seasonal variation. The early summer data from 2010 should reflect the beginning of the growing season, and therefore the minimum SAV coverage. The early fall data from 2014 should reflect the SAV maximum area (Carter et al., 2011). The 2010 areas are larger than the 2014 areas, particularly the West Ship polygon, however. The majority of the SAV polygons from 2010 and 2014 overlap, so both datasets show essentially the same habitable zones (Figure 17). Much of the variation between the 2010 and 2014 polygons may be explained by surveying methodology. SAV extent and patchiness was determined by eye (Barry A. Vittor & Associates, 2011; 2015). All of the SAV areas around Ship Island were patchy, so by definition less than 50% of the polygon

area is actually seagrass area (Figure 18). More detailed survey methods, such as those used by Carter et al., 2011 could improve seagrass monitoring efforts in this area.

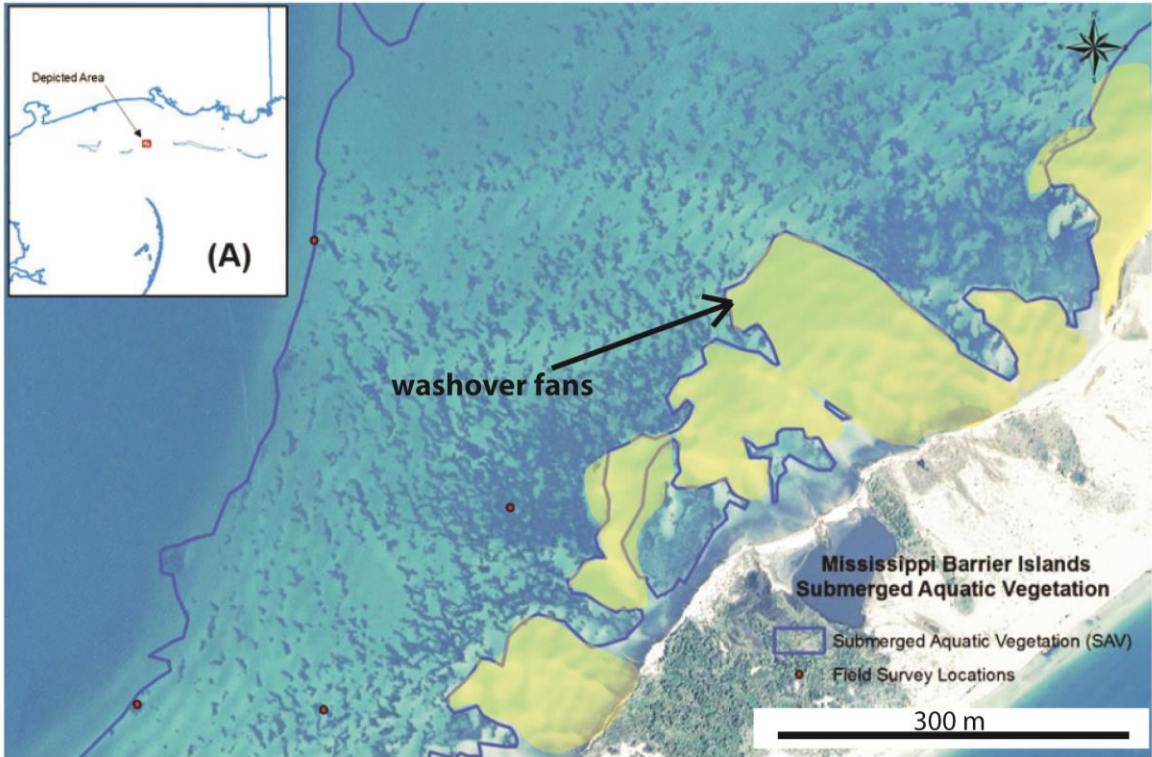


Figure 18. SAV polygon detail.

An up-close example of a polygon drawn around an area of SAV growth from the 2012 survey. Areas highlighted in yellow indicate washover fans. Figure modified from Barry A. Vittor & Associates, 2012.

Sediment Samples

Surface sediment grab samples were collected with the goal of mapping the surface sedimentology around Ship Island, including zones inside and outside of SAV polygons. 45 sediment grab samples were obtained on August 19, 2015 (Figure 19). Grainsize distributions of these samples were measured using a Malvern 3000 Laser Particle Analyzer. D50 and D90 grainsize values were calculated for each sample. Point clouds [longitude, latitude, D50] and [longitude, latitude, D90] were created from these data. They were then gridded to 200 m² cells using a linear interpolation algorithm to

create a digital grainsize model for the shallow bathymetry surrounding Ship Island. The data were gridded within a polygon drawn to contain only areas with available data.

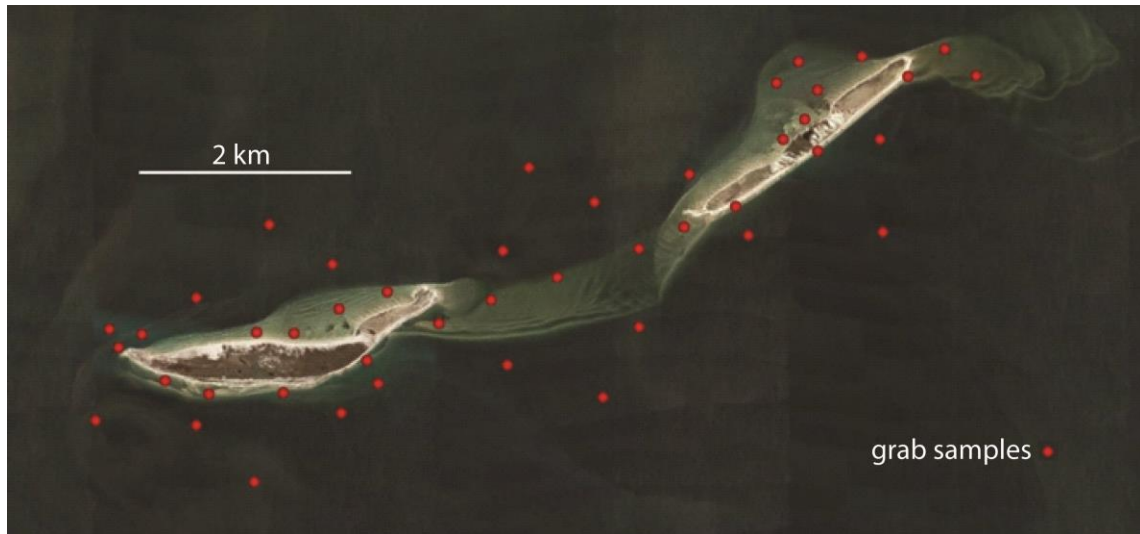


Figure 19. Sediment grab sample locations.

Grab samples were taken from the surface layer of sediments surrounding East and West Ship Islands. Samples were obtained in August 2015 at the locations indicated by red markers on the satellite image above.

Turbidity

Turbidity was measured at 24 locations around East Ship Island, West Ship Island, and in Camille Cut. The data was collected in depth casts using a LISST-100X turbidity meter manufactured by Sequoia Scientific Inc. Turbidity values in and around SAV polygons did not vary significantly. Fair-weather waves in the shallows around Ship Island are not enough to entrain and create significant turbidity with the sandy sediments.

Analysis

Suitable conditions for SAV growth around Ship Island, Mississippi were defined using the SAV polygons, grainsize grids, digital elevation models (DEM's), and difference grids. DEM's and difference grids were derived from topo/bathy LiDAR data of the island. These allowed better definition of what substrate conditions, depths, and

rates of erosion or deposition the SAV in this area can tolerate. SAV shape files were converted to text format, and imported to MATLAB® as polygons. The SAV polygons were used to calculate average depths of each patch using the 2012 LiDAR DEM, and average depth changes over the period 2010 to 2012 from the difference grids. Maximum, minimum, and average grainsize values within the SAV polygons are also calculated.

Results

SAV Distribution

Seagrass. SAV surveys were conducted around East and West Ship Island in 2010 and 2014. One species of seagrass, *Halodule wrightii* Ascherson, or shoal grass, appeared primarily on the north sides of the islands (Figure 17). *H. wrightii* coverage was approximately 1.6 km² across the two islands in 2010 and 1.3 km² in 2014 where West Ship lost 0.7 km² and East Ship gained 0.4 km² (Barry A. Vittor & Associates, 2011; 2015). The East Ship patch is considerably larger in both surveys (Figure 17). The zones of seagrass growth remained mostly consistent from 2010 to 2014, and the area changes are small enough to consider the seagrass distribution stable (Barry A. Vittor & Associates, 2015). One new patchy area of seagrass was mapped in the old western Camille Cut channel in 2014. The 2014 polygons are used for analyses here (Figure 20). All of the seagrass observed was patchy, covering <50% of the area included in the reported SAV extent. The actual seagrass coverage is, therefore, less than half of the reported values.

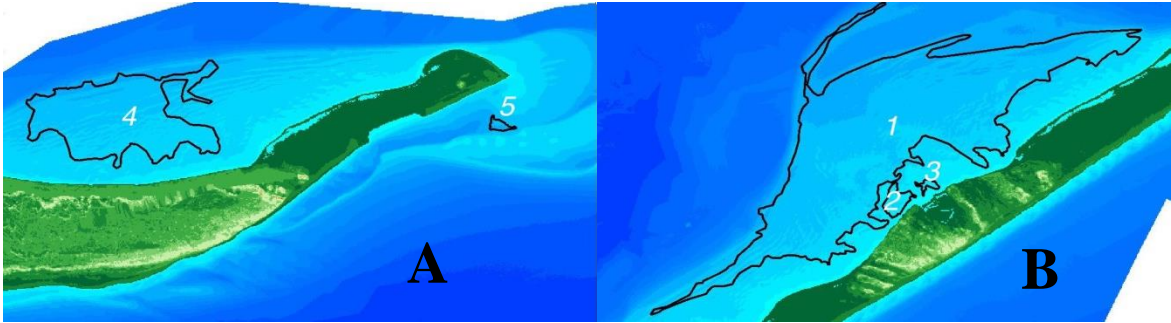


Figure 20. Seagrass polygons.

Polygons around West Ship Island are shown in panel A, and polygons around East Ship Island are shown in panel B. Each patch is labeled with a number.

Macroalgae and Bryozoans. No other SAV species were observed around the islands in 2010, but in 2014, red and brown algae was observed growing alone in patches around West Ship Island and in Camille Cut (Barry A. Vittor & Associates, 2015).

Seagrass patches were all mixed with algae and bryozoan colonies. It was clinging to the seagrass in the West Ship Island patches (Figure 17). A large patch composed solely of the algae was mapped in Camille Cut. The algae patch covered an area of 1.39 km² in 2014. Seagrass beds commonly are associated with drift algae, including red & brown algae like that observed in Camille Cut. These can be important to the seagrass community, and are not necessarily harmful (Dawes, 1987).

Grainsize

Sediment samples for grainsize analysis were obtained from water depths of <1 m to 9 meters around the islands and in Camille Cut. The samples ranged in mean (D50) grain size from 17.4 to 481.6 μm, or silt to medium sand respectively. The D90 values ranged from 94.4 to 803.5 μm, or very fine sand to coarse sand respectively. The coarsest samples (D50 >400 μm) exist in patches in Camille Cut and behind East Ship Island (Figure 21). The finest samples (D50 < 100 μm) were collected far offshore to the south

of West Ship Island (Figure 19). Average erosion/deposition rates were compared with grainsize data where the two overlapped, and no significant correlation was found across the island.

Table 7

Grainsize Data

	Ave D90	Ave D50	Max D90	Min D90	Max D50	Min D50
ES Large Patch	610	388	770	320	467	155
WS Large Patch	530	316	590	430	363	242
OVERALL	458	269	804	94	482	17

Average grainsize data (μm) for the two largest patches of seagrass (patches 1 and 4). Overall grainsize statistics shows average values for all samples taken around Ship Island, both inside and outside areas with SAV.

Within the seagrass polygons, the range of D50 grainsize was 155-467 μm .

Compared with the overall range of D50 grain sizes, the seagrass exists on the coarser sediment. The patches mapped on East Ship Island are coarser than those on West Ship, but both are still in the medium sand range. The finest sediments seagrass was observed growing in had a D50 of 155 μm (fine sand), and the coarsest was a D50 of 467 μm (medium sand).

Bathymetry and Bathymetric Change

Seagrass beds are only observed growing in geomorphologically specific areas around East and West Ship Island. The patches exist on the shallow platforms extending into the Mississippi Sound to the north of the islands (Figure 17, 21). The seagrass is found at depths between ~0.5 m to 2 m (Table 8). Bathymetry changes within the seagrass patches from 2010 to 2012 indicate very minimal change when compared with

areas of rapid erosion/deposition around the islands described in chapter 1 (Table 8).

There is slight erosion in some of the patches, but never occurring at a rate higher than 10 cm/yr.

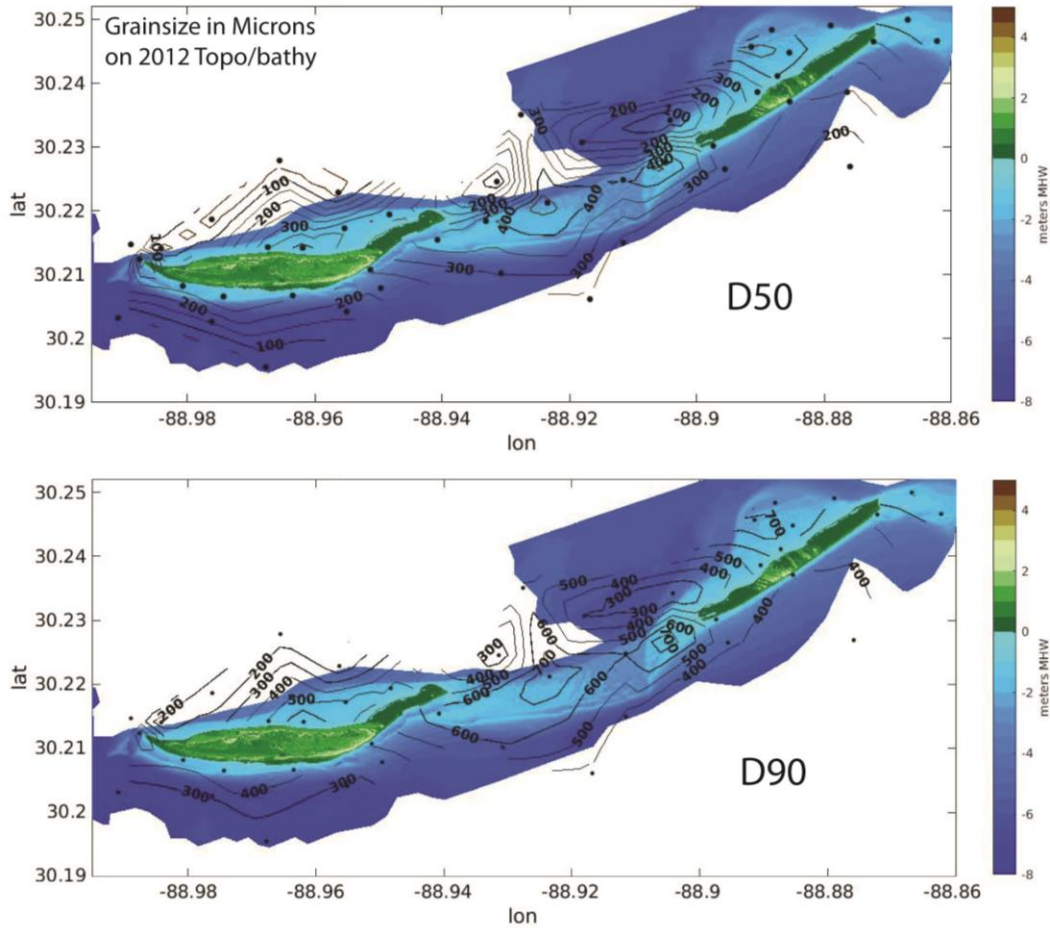


Figure 21. Grainsize contours on topo/bathy DEM.

D50 (panel A) and D90 (panel B) grainsize values (μm) are contoured around Ship Island. The contours are superimposed on the gridded 2012 LiDAR topo/bathy data.

Discussion

Bathymetry

The seagrass growth pattern mapped in 2010 and 2014 is at least partially controlled by bathymetry. Patches of seagrass typically exist at ~ 1.5 m or less, with one

patch growing at ~2 m. This can be explained by light limitation (Iverson & Bittaker, 1986). The Mississippi Sound to the north of the islands is a deeper and muddier

Table 8

Seagrass Patch Areas and Elevations

	Area (m ²)	Average Elevation (m)		Average Change (m/yr)
		2010	2012	
ES patches				
1	9.46E+05	-1.66	-1.68	~0
2	1.49E+04	-0.71	-0.89	-0.09
3	3.91E+03	-0.53	-0.74	-0.10
Totals/Ave	9.65E+05	-0.97	-1.10	-0.06
WS patches				
4	3.03E+05	-1.55	-1.59	~0
5	5.08E+03	-2.03	-2.00	~0
WS Totals	3.08E+05	-1.79	-1.80	~0

Area in square meters of each patch are listed here along with the average elevations within each patch from LiDAR topo/bathy datasets collected in 2010 and 2012 (meters MHW). The comparison of elevations between these two years provides an idea of how much erosion or deposition the seagrass patches are experiencing. The difference between these two years is reported here as well. Most difference values are approximately zero, indicating negligible bathymetric change.

environment, making bottom conditions unsuitable for photosynthetic organisms like seagrass. The sediment on these shallow shelves is within the zone of active sediment transport, and exclusively sandy, reducing sediment-derived turbidity, and allowing better light penetration. This is primarily the reason the seagrass only appears in areas of fine sand and coarser. The seagrass itself is not limited by the grain size of its bottom substrate (Iverson & Bittaker, 1986).

Erosion/Deposition Patterns

LiDAR datasets from 2004 to 2012 show that the backbarrier shallow platform zones, where the majority of seagrass patches exist, has not experienced rapid erosion or deposition over this period. The seagrass is observed tolerating rates of erosion/deposition on the order of 10 cm or less in its current environment around Ship Island (Figure 22). The aerial photographs reveal overwash deposits on the north shore of East Ship Island (Figure 18). These features are devoid of SAV in both 2010 and 2012 surveys. This may indicate that rapid overwash deposition is not favorable for SAV growth/sustainability.

Exposure to Waves

In the Northern Gulf of Mexico the prevailing wind direction is from the southeast. The highest energy fair-weather waves typically impact on the southern shore for this reason. This concentration of high energy is verified by the steeper southern shoreface observed in the bathymetry, and the presence of wide shallow platforms on the north side of the islands (Figure 20). Seagrass is unable to establish in zones regularly exposed to high-energy waves (Iverson & Bittaker, 1986). Protection from waves is important for seagrass growth and establishment, and loss of protective sand bars is shown to have a negative relationship with seagrass area (Fonseca et al., 2002). The formation of bars in the western Camille Cut channel formed a zone protected enough for seagrass to establish between the 2010 and 2012 surveys. This zone is deeper than the other seagrass patches at ~2 m, indicating that where there is sufficient protection and low turbidity, seagrass can grow in greater depths.

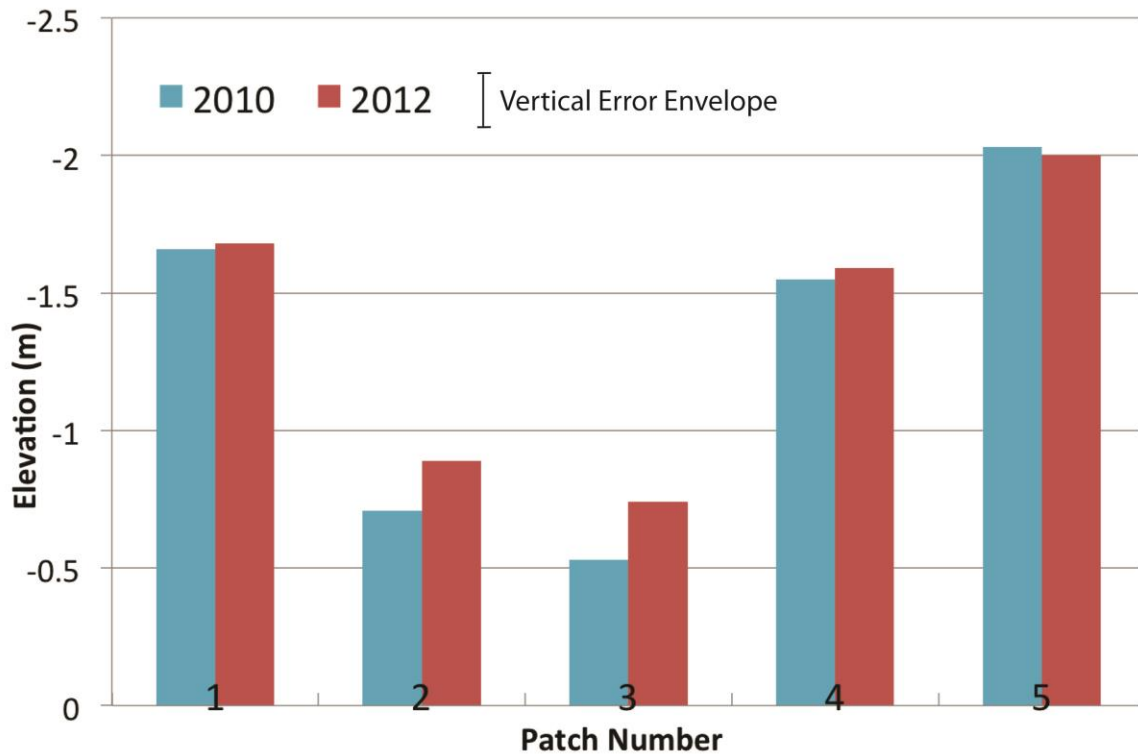


Figure 22. Patch elevations.

Patch elevations are shown here comparing 2010 and 2012 bathymetric data for the areas where seagrass was mapped in 2011/2014. An uncertainty of 0.23 m is applied based on the LiDAR dataset bias.

Algae

The red and brown macroalgae patch observed in Camille Cut in 2012 appears to have a high tolerance for wave exposure. It grows in an area that is directly impacted by the prevailing wave direction from the southeast (Figure 17). Seagrass is unable to colonize this area. Algae and bryozoans, like those found in these surveys, do not necessarily negatively impact seagrass growth and habitat, but can block light in some instances of overgrowth (Huges et al., 2004).

Projected Effectiveness of Camille Cut Restoration

Seagrass around Ship Island almost exclusively grows on the shallow platforms north of the islands. Restoring the central portion of the island may increase area suitable

for seagrass growth, in addition to perhaps providing protection against inland storm surge effects. Management of coastal resources aimed at protecting citizens living along the coast is critical, and public policy and management decisions should reflect this (Dolan and Wallace, 2012).

In the MS/AL barrier chain, the larger the island providing protection from waves, the larger the seagrass patches (Pham et al., 2014). Sandbars placed near Tampa Bay were found to be very effective at increasing seagrass habitat primarily when bars were emergent during some part of the tidal cycle (Fonseca et al., 2002). The effectiveness of a Camille Cut restoration for this purpose will depend on several factors.

The physical stability of the infill is important for maintaining the protected zone behind the islands. This will depend upon the grainsize of the material used and the elevation to which it is built up. The current MsCIP restoration plan considers material with a $D_{50} \geq 280 \mu\text{m}$ sufficient for Camille Cut infill (USACE, 2011). Shore-face and Camille Cut grain sizes are $D_{50} > 300 \mu\text{m}$ in most places. D_{90} values often reach above $700 \mu\text{m}$, very coarse sand, indicating regular exposure to high-energy currents and waves, which the new fill would need to withstand. If the material used is unstable, or built to insufficient elevation, it may be vulnerable to overwash during storm events. Not only can this cause permanent breaches and instability in the island, even if a new inlet is not formed, washover deposits can cover existing seagrass beds along the backbarrier (Figure 18). Material stability may be increased by placing material updrift along the coastline and allowing sediments to deposit naturally in the cut. This will prevent unstable grain sizes from depositing by allowing smaller grain sizes to naturally continue westward to a lower-energy location.

Steepness of the drop off behind Camille Cut may presents a problem, as the seagrass prefers the shallow environment (<2 m around Ship Island). Placing seagrass patches too close to the back barrier beach may leave them vulnerable to smothering by overwash. Construction of a wide back-barrier platform can provide enough area for seagrass to grow at a sufficient distance from the backshore to reduce the risk of washover. The shallow bathymetry of Camille Cut drops off steeply into the Mississippi Sound, in contrast with the shallow shelves that exist north of the main islands. Construction of a feature like this north of the restoration area will require enough sediment to fill the deep area north of Camille Cut.

Once the proper environment for seagrass is established, the grass may begin to increase in area naturally. Seagrass beds were observed to recover at a rate of $\sim 2 \text{ km}^2$ per year in Tampa Bay once management strategies were put in place (Yates et al., 2011). Seagrass coverage in the Tampa Bay area is on the order of 140 km^2 , however, so when scaled to the present seagrass coverage, recovery is only a little more than 1% per year. Ship Island currently only supports about 1.3 km^2 of seagrass coverage (Barry A. Vittor & Associates, 2015). This is the area of polygons drawn around patchy seagrass beds, indicating <50% of the polygon is actual seagrass. This inflated value can become problematic when estimating recovery rates and ecosystem health (Pham et al., 2014). Assuming this was solid seagrass coverage, and it recovers at the same rate as the seagrass observed in Tampa Bay, it would only gain $\sim 0.02 \text{ km}^2$ per year. Natural seagrass bed recovery after loss is typically very slow, and the best approach is often planting (Byron & Heck, 2006; Yates et al., 2011). Nutrient addition via increasing bird perches or other methods will not be necessary as seagrasses require relatively low levels of

nutrients, and increased concentration is correlated with seagrass limitation due to epiphyte growth on the leaves (Hughes et al., 2004).

Conclusions

- I. The three primary limiting factors for seagrass growth in the shallow water around Ship Island Mississippi are wave energy, depth, and rapid deposition, in order of importance.
- II. Seagrass growth around Ship Island, Mississippi is not limited by grainsize and does not encounter limiting levels of turbidity.
- III. Providing a wide, shallow platform protected by the Camille cut restoration material will likely provide a good environment for seagrass growth. Supplemented by plantings, the patches should recover quickly where they are not influenced by overwash events.
- IV. Future studies of SAV growth should be conducted using survey methods that only include area within individual patches rather than large areas with <50% coverage. Digital image analysis methods similar to those employed by Carter et al., 2011 would provide more informative data that is also comparable with most other published datasets.

REFERENCES

- Anderson, J.B., Wallace, D.J., Simms, A.R., Rodriguez, A.B., and Milliken, K.T., 2014. Variable Response of Coastal Environments of the Northwestern Gulf of Mexico to Sea-Level Rise and Climate Change: Implications for Future Change. *Marine Geology*, 352, 348-366.
- Anderson, J.B., Milliken, K.T., Wallace, D.J., Rodriguez, A.B., and Simms, A.R., 2010. Coastal impact underestimated from rapid sea level rise. *Eos Transactions American Geophysical Union*, 91, 205-206.
- Ashton, A.D., and Murray, A.B., 2006. High-angle wave instability and emergent shoreline shapes. Wave climate analysis and comparisons to nature. *Journal of Geophysical Research*. 111, 1-17. <http://doi.org/10.1029/2005JF000423>
- Bird, E.C.F., 1985, *Coastline Changes: A Global Review*: Chichester, UK, Wiley, 219 p.
- Bird, E.C.F., 1996, *Beach Management*: Chichester, UK, Wiley, 281 p.
- Brutsché, K.E., Rosati, J. III, and Pollock, C. E., 2014. Calculating depth of closure using WIS hindcast data. ERDC/CHL CHETN-VI-XX. Vicksburg, MS: U.S. Army Engineer Research and Development Center.
- Buijsman, M.C., Sherwood, C.R., Gibbs, A.E., Gelfenbaum, G., Kaminsky, G., Ruggiero, P., and Franklin, J., 2003. Regional Sediment Budget of the Columbia River Analysis of Bathymetric and Topographic Volume Change. USGS Open-File Report 02-281.
- Byrnes, M.R., Rosati, J.D., Griffee, S.F., & Berlinghoff, J.L., 2012. Littoral sediment budget for the Mississippi Sound Barrier Islands: Mississippi Coastal Improvements Program (MsCIP). http://doi.org/10.1142/9789814355537_0177

- Byrnes, M.R., Rosati, J.D., Griffee, S.F., and Berlinghoff, J.L., 2013. Historical Sediment Transport Pathways and Quantities for Determining an Operational Sediment Budget: Mississippi Sound Barrier Islands. *Journal of Coastal Research*, 63, 166-183. <http://doi.org/10.2112/SI63-014.1>
- Byron, D., and Heck, K.L., Jr., 2006. Hurricane Effects on Seagrasses Along Alabama's Gulf Coast. *Estuaries and Coasts*, 29(6), 939-942.
- Cai, H., Savenije, H., Yang, Q., Ou, S., and Lei Y., 2012. Influence of river discharge and dredging on tidal wave propagation: Modaomen Estuary Case. *Journal of Hydraulic Engineering*, 138, 885-896.
[http://dx.doi.org/10.1061/\(ASCE\)HY.1943-7900.0000594](http://dx.doi.org/10.1061/(ASCE)HY.1943-7900.0000594)
- Carter, G.A., Lucas, K.L., Biber, P.D., Criss, G.A., and Blossom, G.A., 2011. Historical changes in seagrass coverage on the Mississippi barrier islands, northern Gulf of Mexico, determined from vertical aerial imagery (1940–2007). *Geocarto International*, 26(8), 663-673. <http://doi.org/10.1080/10106049.2011.620634>
- Chernetsky, A.S., Schuttelaars, H.M., and Talke, S.A., 2010. The effect of tidal asymmetry and temporal settling lag on sediment trapping in tidal estuaries. *Ocean Dynamics*, 60, 1219-1241.
- Church, J.A., Clark, P.U., Cazenave, A., Gregory, J.M., Jevrejeva, S., Levermann, A., Merrifield, M.A., Milne, G.A., Nerem, R.S., Nunn, P.D., Payne, A.J., Pfeffer, W.T., Stammer, D., and Unnikrishnan, A.S., 2013. Sea Level Change: Climate Change 2013: The Physical Science Basis. Contribution of Working Group I to the Fifth Assessment Report of the IPCC. Cambridge University Press.

- Church, J.A., and White, N.J., 2006. A 20th century acceleration in global sea-level rise. *Geophysical Research Letters*, 33. doi:10.1029/2005GL024826.
- Dawes, C. J., 1987. The dynamic seagrasses of the Gulf of Mexico and Florida Coasts. Florida Department of Natural Resources, Bureau of Marine Research. St. Petersburg, FL. *Florida Marine Research Publications*, 42, 25-52.
- Dolan, G. and Wallace, D.J., 2012. Policy and Management Hazards along the Upper Texas Coast. *Ocean & Coastal Management*, 59, 77-82.
- Eleuterius, L., 1987. Seagrass ecology along the coasts of Alabama, Louisiana, and Mississippi. *Florida Marine Research Publications*, 11-24.
- FitzGerald, D.M., Buynevich, I.V., and Argow, B., 2006. Model of tidal inlet and barrier island dynamics in a regime of accelerated sea-level rise. *Journal of Coastal Research*, 39, 789-795.
- FitzGerald, D. M., Fenster, M. S., Argow, B.A., Buynevich, I.V., 2008. Coastal Impacts Due to Sea-Level Rise. *Annual Review of Earth and Planetary Sciences*, 36, 601-47.
- Fonseca, M. S., Robbins, B. D., and Whitfield, P. E., 2002. Evaluating the effect of offshore sandbars on seagrass recovery and restoration in Tampa Bay through ecological forecasting and hindcasting of exposure to waves. NOAA Report. Tampa Bay Estuary Program.
- Fritz, H.M., Blount, C., Sokoloski, R., Singleton, J., Fuggle, A., McAdoo, B.G., Moore, A., Grass, C., and Tate, B., 2007. Hurricane Katrina storm surge distribution and field observations on the Mississippi Barrier Islands. *Estuarine, Coastal and Shelf Science*, 74(1), 12-20.

- González, J. L., and Törnqvist, T. E., 2009. A new Late Holocene sea-level record from the Mississippi Delta: evidence for a climate/sea level connection? *Quaternary Science Reviews*, 28(17–18), 1737–1749.
<http://doi.org/10.1016/j.quascirev.2009.04.003>
- Handley, L., Altsman, D., and DeMay, R., 2007. Seagrass status and trends in the northern Gulf of Mexico: 1940-2002 (Report Version 1.). Scientific Investigations Report. Reston, VA. URL: <http://pubs.er.usgs.gov/publication/sir20065287>
- Hughes, A.R., Bando, K.J., Rodriguez, L.F., Williams, S.L., 2004. Relative effects of grazers and nutrients on seagrasses: a meta-analysis approach. *Marine Ecology Progress Series*, 282, 87–99.
- Isenburg, M., 2015. M. LAStools - efficient LiDAR processing software (version 141017, unlicensed). <http://rapidlasso.com/LAStools>.
- Iverson, R.L., and Bittaker, H.F., 1986. Seagrass distribution and abundance in Eastern Gulf of Mexico coastal waters. *Estuarine, Coastal and Shelf Science*, 22(5), 577-602. [http://doi.org/10.1016/0272-7714\(86\)90015-6](http://doi.org/10.1016/0272-7714(86)90015-6)
- Jiang, C., J. Li, and de Swart, H.E., 2012. Effects of navigational works on morphological changes in the bar area of the Yangtze Estuary. *Geomorphology*, 139, 205-219.
- McBride, R.A., Anderson, J.B., Buynevich, I.V., and 14 others, 2013. Morphodynamics of barrier systems: a synthesis. In: Shroder, J. (Editor in Chief), Sherman, D.J. (Ed.), *Treatise on Geomorphology*. Academic Press, San Diego, CA, *Coastal and Submarine Geomorphology*, 10, 166–244.

- McBride, R.A., and Byrnes, M.R., 1997. Regional Variations in Shore Response along Barrier Island Systems of the Mississippi River Delta Plain: Historical Change and Future Prediction. *Journal of Coastal Research*, 13(3), 628–655.
- Morton, R.A., 2008. Historical Changes in the Mississippi-Alabama Barrier-Island Chain and the Roles of Extreme Storms, Sea Level, and Human Activities. *Journal of Coastal Research*, 24(6), 1587-1600. <http://doi.org/10.2112/07-0953.1>
- NOAA Historical Hurricane Tracks. URL: <https://coast.noaa.gov/hurricanes>. Accessed on October 5, 2016.
- NOAA, 2013. Ship Island, Mississippi Sound, MS tide gauge (#8744756). 1979-2011 tidal epoch. URL: <https://tidesandcurrents.noaa.gov/stationhome.html?id=8744756>. Accessed on October 5, 2016.
- NDBC, 2016. Climatic summary statistics for Station 42007, 1981-2008. URL: http://www.ndbc.noaa.gov/station_page.php?station=42007. Accessed on October 5, 2016.
- Orth, R.J., Carruthers, T.J.B., Dennison, W.C., Duarte, C.M., Fourqurean, J.W., Heck, K.L., Williams, S.L., 2006. A Global Crisis for Seagrass Ecosystems. *BioScience*, 56(12), 987. [http://doi.org/10.1641/0006-3568\(2006\)56\[987:AGCFSE\]2.0.CO;2](http://doi.org/10.1641/0006-3568(2006)56[987:AGCFSE]2.0.CO;2)
- Otvos, E.G., 1978. New Orleans–South Hancock Holocene barrier trends and origins of Lake Pontchartrain. *Gulf Coast Association of Geological Societies, Transactions*, 28, 295-355.
- Otvos, E.G., 2004. Holocene sea-levels: recognition issues and an updated sea-level curve. *Journal of Coastal Research*, 20, 680-699.

- Otvos, E.G., 2005. Validity of sea-level indicators: A comment on “A new depositional model for the buried 4000 yr BP New Orleans barrier: implications for sea-level fluctuations and onshore transport from a nearshore shelf source” by F.W. Stapor and G.W. Stone [*Marine Geology*, 204 (2004), 215–234]. *Marine Geology*, 217, 177-187.
- Otvos, E.G., and Carter, G.A., 2008. Hurricane Degradation - Barrier Development Cycles , Northeastern Gulf of Mexico: Landform Evolution and Island Chain History. *Journal of Coastal Research*, 24(2), 463-478.
<http://dx.doi.org/10.2112/06-0820.1>
- Otvos, E.G., and Carter, G.A., 2013. Regressive and transgressive barrier islands on the North-Central Gulf Coast - Contrasts in evolution, sediment delivery, and island vulnerability. *Geomorphology*, 198, 1-19.
<http://doi.org/10.1016/j.geomorph.2013.05.015>
- Otvos, E.G., and Giardino, M.J., 2004. Interlinked barrier chain and delta lobe development, northern Gulf of Mexico. *Sedimentary Geology*, 169(1-2), 47-73.
<http://doi.org/10.1016/j.sedgeo.2004.04.008>
- Overpeck, J.T., Otto-Bliesner, B.L., Miller, G.H., Muhs, D.R., Alley, R.B., and Kiehl, J.T., 2006. Paleoclimatic evidence for future ice-sheet instability and rapid sea level rise. *Science*, 311, 1747–1750. doi:10.1126/science.1115159
- Pendleton, E.A., Barras, J.A., Williams, S.J., and Twichell, D.C., 2010. Coastal vulnerability assessment of the Northern Gulf of Mexico to sea-level rise and coastal change: U.S. Geological Survey Open-File Report 2010-1146. URL:
<http://pubs.usgs.gov/of/2010/1146/>

- Pfeffer, W.T., Harper, J.T., and O'Neel, S., 2008. Kinematic constraints on glacier contributions to 21st-century sea level rise. *Science*, 321, 1340-1343, doi:10.1126/science.1159099
- Pham, L.T., Biber, P.D., and Carter, G. A., 2014. Seagrasses in the Mississippi and Chandeleur Sounds and Problems Associated With Decadal-Scale Change Detection. *Gulf of Mexico Science*, 32, 24-43.
- Priestas, A. M., and Fagherazzi, S., 2010. Morphological barrier island changes and recovery of dunes after Hurricane Dennis, St. George Island, Florida. *Geomorphology*, 114(4), 614–626. <http://doi.org/10.1016/j.geomorph.2009.09.022>
- Sallenger, A.H., Jr., 2000. Storm Impact Scale for Barrier Islands. *Journal of Coastal Research*, 16(3), 890-895.
- Saucier, R.T., 1963. Recent geomorphic history of Pontchartrain basin. *Louisiana State University Coastal Studies Series*, 9, 114 p.
- Saucier, R.T., 1994. Geomorphology and Quaternary Geologic History of the Lower Mississippi Valley, vol. 1. US Army Corps of Engineers Waterways Experiment Station, Vicksburg, MS.
- Stapor Jr., F.W., Stone, G.W., 2004. A new depositional model for the buried 4000 yr BP New Orleans barrier: implications for sea-level fluctuations and onshore transport from a nearshore shelf source. *Marine Geology*, 204, 215–234.
- Stone, G.W., Liu, B., Pepper, D.A., and Wang, P., 2004. The importance of extratropical and tropical cyclones on the short-term evolution of barrier islands along the

northern Gulf of Mexico, USA. *Marine Geology*, 210(1-4), 63-78.

<http://doi.org/10.1016/j.margeo.2004.05.021>

Thomas, R., Rignot, E., Casassa, G., and 15 others, 2004. Accelerated sea-level rise from West Antarctica. *Science*, 306, 255-258. doi:10.1126/science.1099650.

Törnqvist, T. E., Bick, S. J., van der Borg, K., & de Jong, A. F. M., 2006. How stable is the Mississippi Delta? *Geology*, 34(8), 697-700. <http://doi.org/10.1130/G22624.1>

Törnqvist, T.E., González, J.L., Newsom, L.A., van der Borg, K., de Jong, A.F.M., and Kurnik, C.W., 2004. Deciphering Holocene sea-level history on the U.S. Gulf Coast: A high-resolution record from the Mississippi Delta. *Bulletin of the Geological Society of America*, 116(7-8), 1026-1039.

<http://doi.org/10.1130/B2525478.1>

Twichell, D.C., Flocks, J.G., Pendleton, E.A., and Baldwin, W.E., 2013. Geologic Controls on Regional and Local Erosion Rates of Three Northern Gulf of Mexico Barrier-Island Systems. *Journal of Coastal Research*, 63, 32-45.

<http://doi.org/10.2112/SI63-004.1>

USACE, 1970. Report on Hurricane Camille, 14-22 August 1969. U.S. Army Engineer District, Mobile Corps of Engineers, Mobile, Alabama.

USACE, 2010. Mississippi Coastal Improvements Program (MsCIP) – Barrier Island Restoration Plan: West Ship Island North Shore Restoration, Mississippi Sound, Harrison County, Mississippi. Public Notice No. Fp10-SI01-08.

USACE, 2011. Mississippi Coastal Improvements Program (MsCIP) - Camille Cut Closure, A desk-top analysis of closure options. MsCIP Multi-Agency Meeting.

- USACE, 2014. Mississippi Coastal Improvements Program (MsCIP) – Comprehensive Barrier Island Restoration. Hancock, Harrison, and Jackson Counties, Mississippi. Draft Supplemental Environmental Impact Statement.
- Vittor, B. A. and Associates, Inc., 2011. Mapping of Submerged Aquatic Vegetation in 2010. Final Report. Mississippi Barrier Island Restoration Project.
- Vittor, B. A. and Associates, Inc., 2015. 2014 Mapping of Submerged Aquatic Vegetation. Final Report. Mississippi Coastal Improvements Program (MsCIP).
- Wallace, D.J., and Anderson, J.B., 2013. Unprecedented erosion of the upper Texas Coast: Response to accelerated sea-level rise and hurricane impacts. *Geological Society of America Bulletin*, 125(5-6), 728-740.
- Wallace, D.J., Anderson, J.B., and Fernández, R.A., 2010. Transgressive Ravinement versus Depth of Closure: A Geological Perspective from the Upper Texas Coast. *Journal of Coastal Research*, 26(6), 1057-1067.
- Waller, T.H. and Malbrough, L.P., 1976. Temporal Changes in the Offshore Islands of Mississippi. Mississippi State, Mississippi: Mississippi State University Water Resources Institute.
- Walstra, D.J.R, de Vroeg, J.H., van Thiel de Vries, J.S.M.; Swinkels, C., Lujendijk, A.P., de Boer, W.P., Hoekstra, R., Hoonhout, B., Henrotte, J., Smolders, T., Dekker, F., Godsey, E., 2012. A Comprehensive Sediment Budget for the Mississippi Barrier Islands. ICCE 2012: Proceedings of the 33rd International Conference on Coastal Engineering.
- Waple, A., 2005. Hurricane Katrina: NOAA's National Climatic Data Center, Asheville, NC.

Yates, K.K., Morrison, G., and Greening, H., 2011. Seagrass: Integrating Science and Resource Management in Tampa Bay, Florida, 63–104. URL:

<http://pubs.usgs.gov/circ/1348/>

Zhu, J., Weisberg, R.H., Zheng, L., and Han, S., 2015. Influences of channel deepening and widening on the tidal and nontidal circulations of Tampa Bay. *Estuaries and Coasts*, 38(1), 132-150.